HYPERSONIC AEROSPACE VEHICLE LEADING EDGE COOLING USING HEAT PIPE, TRANSPIRATION AND FILM COOLING TECHNIQUES

A THESIS
Presented to
The Academic Faculty

by

James Michael Modlin

In Partial Fulfillment
of the Requirements for the Degree
Doctor of Philosophy in Mechanical Engineering

Georgia Institute of Technology
June 1991

REPORT DOCUMENTATION PAGE

Form Approved
OMB No. 0704-0188

1. AGENCY USE ONLY (Leave Blank)	2. REPORT DATE	3. REPORT TYPE AND DATES COVERED
	JUNE 1991	PH.D THESIS

4. TITLE AND SUBTITLE
HYPERSONIC AEROSPACE VEHICLE LEADING EDGE COOLING USING HEAT PIPE, TRANSPIRATION AND FILM COOLING TECHNIQUES

5. FUNDING NUMBERS

6. AUTHOR(S)
JAMES M. MODLIN

7. PERFORMING ORGANIZATION NAME(S) AND ADDRESS(ES)

8. PERFORMING ORGANIZATION REPORT NUMBER

9. SPONSORING/MONITORING AGENCY NAME(S) AND ADDRESS(ES)
DEPARTMENT OF THE ARMY
U.S. TOTAL ARMY PERSONNEL COMMAND
ALEXANDRIA, VA 22332-0415

10. SPONSORING/MONITORING AGENCY REPORT NUMBER

11. SUPPLEMENTARY NOTES
A THESIS COMPLETED IN PARTIAL FULFILLMENT OF THE REQUIREMENTS FOR THE DEGREE OF DOCTOR OF PHILOSOPHY

12a. DISTRIBUTION/AVAILABILITY STATEMENT
PUBLIC

12b. DISTRIBUTION CODE

13. ABSTRACT (Maximum 200 words)
AN INVESTIGATION WAS CONDUCTED TO DETERMINE THE FEASIBILITY OF USING LIQUID METAL HEAT PIPE, TRANSPIRATION AND FILM COOLING TECHNIQUES TO COOL AEROSPACE VEHICLE LEADING EDGE STRUCTURES EXPOSED TO SEVERE, TRANSIENT HYPERSONIC FLIGHT AERODYNAMIC HEATING ENVIRONMENTS. A FINITE-DIFFERENCE, NUMERICAL COOLING MODEL WAS DEVELOPED AND APPLIED TO AN AEROSPACE PLANE WING LEADING EDGE SECTION AND TO A SCRAMJET INLET SECTION. IT WAS DEMONSTRATED THAT THESE COOLING TECHNIQUES ARE FEASIBLE.

14. SUBJECT TERMS
NATIONAL AEROSPACE PLANE, HEAT TRANSFER, HYPERSONIC, HEAT PIPE, TRANSPIRATION, FILM COOLING, SCRAMJET

15. NUMBER OF PAGES
116

16. PRICE CODE

17. SECURITY CLASSIFICATION OF REPORT	18. SECURITY CLASSIFICATION OF THIS PAGE	19. SECURITY CLASSIFICATION OF ABSTRACT	20. LIMITATION OF ABSTRACT
UNCLAS	UNCLAS	UNCLAS	

HYPERSONIC AEROSPACE VEHICLE LEADING EDGE COOLING USING HEAT PIPE, TRANSPIRATION AND FILM COOLING TECHNIQUES

APPROVED:

Gene T. Colwell, PhD, Chairman

William Z. Black, PhD

James G. Hartley, PhD

James C. Wu, PhD

Charles W. Gorton, PhD

Date Approved by Chairman: 4-29-91

ACKNOWLEDGEMENT

It is with sincere appreciation and thanks that those outstanding individuals who truly made this work possible are duly acknowledged. The author is greatly indebted to Professor Gene T. Colwell for the many months of patience, guidance and invaluable assistance he has provided as both a teacher and an advisor. Without his keen insight and depth of engineering expertise the accomplishment of this study would have been significantly hindered. The author is proud to consider Professor Colwell a professional colleague and friend.

Additionally, the author wishes to thank Professors William Z. Black, James G. Hartley, James C. Wu and Charles W. Gorton for their consideration and assistance as members of the thesis reading committee. Their suggestions and advice have added greatly to the quality of this work. Further, the general support and guidance given the author throughout his doctoral studies at Georgia Tech by Professors Prateen V. Desai, William J. Wepfer, and Ward O. Winer is truly appreciated.

Appreciation is also extended to the United States Department of the Army for their faith, confidence and support in the author's desire and abilities to continue his professional education while serving on active duty in the Army.

Most importantly, it is with heart-felt love, affection and thanks that the author acknowledges the invaluable and unselfish support he received from his wife Cindy and his four sons Jim, Matt, Dan and Josh throughout this challenging period of their lives. Without them, none of this would have been possible . . . to them, this work is dedicated.

LIST OF TABLES

TABLE OF CONTENTS

LIST OF FIGURES

NOMENCLATURE

Variables

a	speed of sound [m/sec]
C	specific heat [kJ/kg-K]
Cp	constant pressure specific heat [kJ/kg-K]
c_f	coefficient of friction
HP	heat pipe
L	heat pipe length
ℓ	unit span length
M	molecular weight [kg/kmol]
Ma	Mach number
m	mass [kg]
$\dot{m}$	mass flowrate [kg/sec]
Pr	Prandtl number
Q	heat transfer rate [W]
q	heat flux [W/m^2]
Re	Reynolds number
St	Stanton number
T	temperature [K]

t	time [sec]
u	chordwise direction flow velocity [m/sec]
v	normal direction flow velocity [m/sec]
x	chordwise direction
y	normal direction
z	spanwise direction

Greek Variables

β	shock wave angle
γ	specific heat ratio
Δ	leading edge sweep angle
ϵ	surface emissivity
θ	leading edge wedge half-angle
κ	thermal conductivity [W/m-K]
μ	viscosity [N-sec/m^2]
ρ	density [kg/m^3]
σ	Stefan-Boltzmann Constant [W/m^2-K^4]

Subscripts

AERO	aerodynamic
AIR	air property

COOL	coolant property
e	boundary layer edge condition
FP	flat plate
HX	heat exchanger
NOSE	aircraft nose
o	no surface cooling condition
os	outer surface
RAD	radiation
r	recovery condition
SP	stagnation point
STAG	stagnation condition
scs	heat pipe skin/capillary structure interface
V	vapor
VIN	into vapor
VOUT	from vapor
w	wall/surface condition
1	heat pipe skin
2	heat pipe capillary structure, conditions after vehicle nose shock
3	conditions after engine inlet bow shock
∞	surroundings condition

SUMMARY

An investigation was conducted to study the feasibility of cooling hypersonic vehicle leading edge structures exposed to severe aerodynamic surface heat fluxes using a combination of liquid metal heat pipes and surface mass transfer cooling techniques. A generalized, transient, finite difference based hypersonic leading edge cooling model was developed which incorporated these effects and was demonstrated on an assumed aerospace plane-type wing leading edge section and on a SCRAMJET engine inlet leading edge section.

The hypersonic leading edge cooling model of this study was developed using an existing, experimentally verified finite difference based heat pipe model. The existing heat pipe model was modified by adding transpiration and film cooling options as new surface boundary conditions. The models used to predict the transient leading edge surface heat transfer reduction effects due to the transpiration and film cooling were generalized, empirically based models obtained from the literature. They, in turn, required further modification to better adapt to the specific needs of this study and for use in conjunction with the existing finite difference leading edge heat pipe model.

Two applications of the hypersonic leading edge cooling model were examined. First, an assumed aerospace plane-type wing leading edge section exposed to a severe laminar, hypersonic aerodynamic surface heat flux was studied. In the model a one inch

nose diameter leading edge structure was cooled using a lithium filled heat pipe supplemented by either surface transpiration, surface film, or internal active heat exchanger cooling while executing a 2000 psf constant dynamic pressure hypersonic ascent flight trajectory through the Earth's atmosphere. Surface coolants used in the study were gaseous air, helium and water vapor. The results of applying the cooling model to the hypersonic wing leading edge case included transient structural temperature distributions, transient aerodynamic heat inputs, and transient surface coolant distributions. The results of this application indicated that these cooling techniques limited the maximum leading edge surface temperatures and moderated the structural temperature gradients.

A second application of the hypersonic leading edge cooling model was conducted on an assumed one-half inch nose diameter SCRAMJET engine inlet leading edge section exposed to a transient laminar, hypersonic aerodynamic surface heat flux and Type IV shock interference surface heating. In this model the leading edge structure was again cooled using a lithium filled heat pipe but only supplemented by either air transpiration or film cooling. Similar results reported for the wing leading edge case were reported for this application. The results indicated that the combination of liquid metal heat pipe cooling and surface transpiration or film cooling tended to mitigate the otherwise severe maximum leading edge surface temperatures expected on a SCRAMJET engine inlet structure exposed to a typical hypersonic flight environment and shock interference effects.

Thus, the results of this investigation led to the conclusion that cooling leading edge structures exposed to a hypersonic environment using a combination of liquid metal heat pipe and surface mass transfer cooling methods appears feasible and that further study/experimental investigations are required to validate these predicted results.

CHAPTER I

INTRODUCTION

The need for developing a more economical access to space and increased commercial global transportation demands has stimulated renewed international interest in the development of a hypervelocity, airbreathing aerospace vehicle during recent years. By providing short launch requirements and rapid turnaround times, these vehicles could have the responsive, flexible operational characteristics approaching those of today's aircraft and could eventually replace the space shuttle. It is envisioned that one version of this vehicle would be able operate in a low-Earth orbit, while another version would remain in the Earth's atmosphere transporting passengers or cargo to any location in a fraction of the time required for current jet aircraft travel.

The embodiment of the hypervelocity vehicle concept in the United States is the joint NASA/Department of Defense National Aerospace Plane (NASP) Program. This program considers of interest both hypersonic cruise and accelerator type vehicles. Unlike the space shuttle, these vehicles would takeoff and land on standard runways, operate within an airbreathing corridor of the atmosphere and be powered by airbreathing

engines. A gas turbine jet-engine would provide the thrust for takeoff and acceleration to supersonic velocities, RAMJETS would be used for acceleration to Mach 5 and SCRAMJETS for acceleration to Mach 20 or above. Some of the vehicles would be designed to ascend to an altitude of twenty or more miles above the Earth and cruise at hypersonic speeds of Mach 6 to 12. Others would be designed to continue accelerating through an airbreathing corridor to Mach 25 and, with minimal rocket power, transition to a low-Earth orbit.

The space shuttle uses significant rocket power to enter a low-Earth orbit in a relatively short period of time. The airbreathing propulsion system for the aerospace plane, though, will require long acceleration periods within the denser part of the Earth's atmosphere to reach cruise and orbital velocities. This long flight time coupled with the need for a low aerodynamic drag configuration will result in severe aerodynamic heating of the aerospace vehicle's surfaces. At hypersonic velocities air has an enormous amount of kinetic energy. As the air velocity is decreased by the viscous boundary layer action at the vehicle's surface, a large portion of the kinetic energy is converted into internal energy which, in turn, significantly increases the boundary layer air temperature. The greater the magnitude of the air velocity reduction, the more extreme this effect becomes. Therefore, a major engineering consideration in the design of the aerospace vehicle is the determination of the severity of the heat transfer from the heated boundary layer to the surface and the management of this increased heating rate. Especially critical surface locations are at the leading edges of the vehicle's wings, engines, and fuselage.

Thus, at hypersonic flight speeds all leading edges must be blunt-nosed to some extent in order to reduce the heat transfer rates to manageable proportions and to allow for internal heat conduction. However, the proposed aerospace plane will ideally require very sharp leading edge geometries in order to gain the desired propulsion system performance and aerodynamic control. The result will be a marked increase in the expected maximum surface heating rates compared to that experienced by previous hypersonic vehicles. Table 1.1 lists examples of the maximum heat flux data for a wing section of the space shuttle, which occurs upon re-entry, and for an expected wing section of the aerospace plane. Note that the aerospace plane has a maximum wing heat flux one to two orders of magnitude greater than the space shuttle. For the descent/re-entry case this difference is primarily due to the aerospace plane's reduced drag configuration (sharper leading edge). For the ascent case, the sharp leading edge combined with a longer acceleration time in the Earth's atmosphere causes this case to be one of the most critical for the aerospace plane's thermo-structural design.

Also listed in Table 1.1 are the corresponding radiation equilibrium skin temperatures assuming a surface emissivity of 0.85. These temperatures are well above the maximum safety limits of available aero-structural skin materials. Thus, the aerospace vehicle surface, at these intense heating locations, must somehow be protected. Several methods of surface cooling and protection are possible for various geometries. For example, thermal barrier coatings could be attached to outer skins, internal convective cooling could be used as a structural heat sink by circulating the vehicle's cryogenic fuel through

TABLE 1.1. Space Shuttle and NASP Wing Maximum Surface Heating Comparison

CASE	MAXIMUM HEAT FLUX [kW/m^2]	EQUILIBRIUM SKIN TEMPERATURE [K]
SHUTTLE RE-ENTRY	4×10^2	1697
NASP DESCENT	2×10^3	2538
NASP ASCENT	1×10^4	3795

the hot structures, surface mass transfer cooling techniques (transpiration, film, or ablation) could be considered, or liquid metal heat pipes could be placed in critical regions. Each method provides its own strengths and weaknesses, but it now appears that none are individually capable of providing the required surface protection for the aerospace plane during an entire ascent flight mission.

Problem Statement

The design of the hypervelocity aerospace plane requires the solution of a significant number of multi-disciplinary engineering problems. As mentioned, a major concern is the thermal management of the various exposed surface leading edges. This thesis reports on an investigation that was conducted to study one possible method of reducing the structural temperatures of a hypersonic vehicle leading edge.

To date no technique has been developed which adequately cools these leading edge structures when exposed to the expected maximum aerodynamic surface heat fluxes. It appears that combinations of techniques must be investigated in order to develop a satisfactory cooling method. In the present work an analytical study was conducted to determine the feasibility of cooling hypersonic aerospace plane leading edge structures during periods of maximum aerodynamic heating using liquid metal heat pipes supplemented by surface transpiration or film cooling. Although some work has been done previously on heat pipe cooling of hypersonic leading edges, no definitive solution for an aerospace plane-type leading edge has been reported nor has there been any

reference made towards incorporating surface mass transfer cooling with heat pipe cooling as a possible technique. It is envisioned that the results of the present investigation will add to the existing body of knowledge being gathered to determine an optimal aerospace plane leading edge cooling concept.

The specific objectives of the study were:

1. To model the external surface transpiration cooling of an aerospace plane leading edge in series with internal liquid metal heat pipe cooling.

2. To model the external surface film cooling of an aerospace plane leading edge in series with internal liquid metal heat pipe cooling.

3. To evaluate the effectiveness of each cooling concept based upon maximum structural surface temperatures and temperature gradients.

4. To investigate the effectiveness of various surface coolants.

5. To compare objectives 1 through 4 to the corresponding heat pipe alone cooled leading edge and the heat pipe with an active internal heat exchanger only cooled leading edge.

The procedures used to accomplish these objectives are presented in the following chapters. Chapter II discusses the background of this cooling problem. A general description of heat pipe and surface mass transfer cooling is given and a review of the literature on how these techniques have been employed previously to cool hypersonic surfaces is conducted. Chapter III discusses the general analytical models that were used in the investigation to develop a hypersonic leading edge cooling model for studying the leading edge cooling problem. An experimentally verified finite difference numerical heat pipe model is reviewed along with an empirically determined transpiration cooling relationship and a theoretically developed, experimentally checked film cooling relation. These three heat transfer models are modified and combined in Chapter IV. The resultant transient, numerically based hypersonic leading edge cooling model is then applied to the case of cooling an aerospace plane wing leading edge structure exposed to a severe laminar, aerodynamic surface heating environment. To do so certain vehicle geometric and operational characteristics were developed and assumed. An aerodynamic surface heating analysis and a hypersonic flow-field development, to include high temperature air/real gas effects, were required. The results of applying the hypersonic leading edge cooling model to the wing using three gaseous coolants are then presented and discussed. A second application of the cooling model is undertaken in Chapter V. A SCRAMJET engine inlet, exposed to both a severe aerodynamic and Type IV shock interaction surface heating environment, is analyzed using the same techniques developed in Chapter IV. Again, results are presented and discussed. Finally, a summary of the

investigation's significant findings along with pertinent conclusions and recommendations for future study are given in Chapter VI.

Before preceding, however, it must be noted that the underlying theme throughout the conduct of this investigation was the desire to develop a tool for use in further detailed engineering design calculations of hypersonic leading edge cooling. As such, the cooling model developed in this study is intentionally general in order that it may be applied to a variety of hypersonic vehicle leading edge systems, as will be demonstrated in Chapters IV and V. In this investigation emphasis was placed on studying the hypersonic leading edge structural response to severe aerodynamic surface heating effects and on the feasibility of cooling these structures through heat pipe and surface mass transfer techniques. No attempt was made to analyze, in great detail, the complicated hypersonic and surface boundary layer flow-field with mass addition to develop transpiration and film cooling models. Rather, empirically verified results reported in the literature and considered applicable to the problem of interest to this investigation were used.

CHAPTER II

BACKGROUND

This chapter discusses the previous and on-going work of applying liquid metal heat pipe cooling techniques to the problem of cooling a hypersonic aerospace plane leading edge. A general description of the heat pipe operation is presented and the work on using surface mass transfer cooling techniques to cool high speed surfaces is discussed.

General Heat Pipe Description and Operation

A heat pipe is a passive, self-contained heat transfer device which has the capability of transferring large heat fluxes nearly isothermally. The most common form of heat pipe is that of a right circular cylinder geometry as shown in Figure 2.1. However many other geometries are used in practice to suit a particular application, such as the shape of a wing leading edge.

There are three primary components of a heat pipe: the outer shell, the wick or capillary structure, and the working fluid. The outer shell is typically thin in order to promote good conduction heat transfer, but must be structurally sound enough to

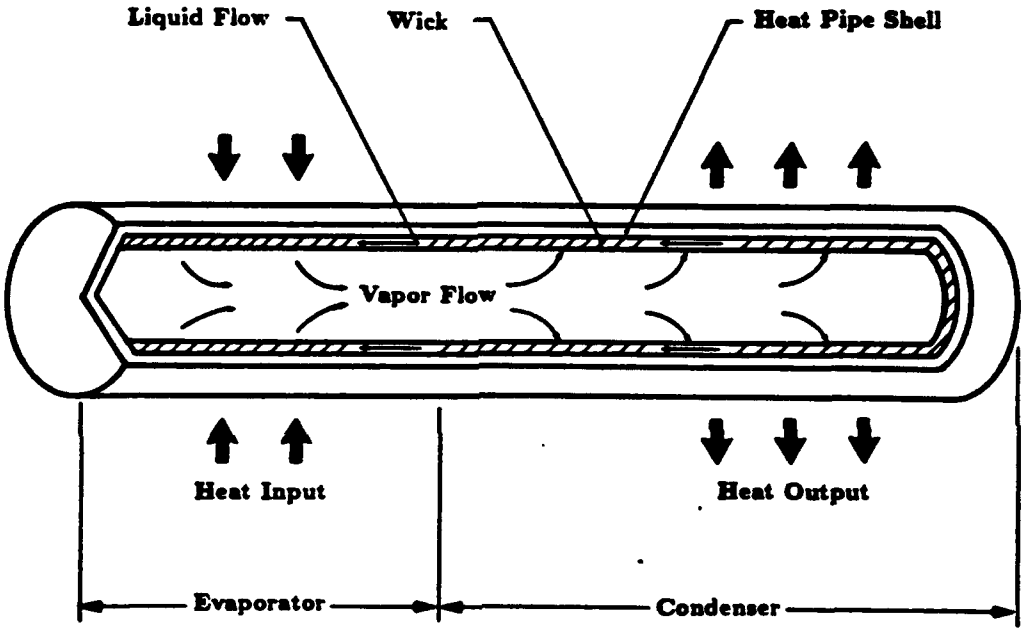

FIGURE 2.1. Schematic of a Cylindrical Heat Pipe Showing Operational Characteristics

withstand maximum operating temperatures and pressures. The wick is a fine mesh/screen material. The open pores within the wick constitute the capillary structure and are filled with the working fluid. Heat pipes have been developed using a variety of working fluids. As shown in Table 2.1, these working fluids have ranged from cryogenic liquids to liquid metals and have allowed the manufacture of a variety of heat pipes that are functional over operating temperatures ranging from 5 K to 2000 K.

The heat pipe operates by vaporizing the working fluid at one end, the evaporator section, and condensing it at the other end, the condenser section. Thus, by utilizing the working fluid's latent heat of vaporization and condensation heat is transferred through the heat pipe nearly isothermally. The working fluid vapor flow is accomplished by the pressure difference created by these phase change processes. The evaporated working fluid in the evaporator section is replenished by fluid returned to it from the condenser section through a capillary pumping action in the wick. This fluid flow mechanism allows the heat pipe to be operated in a variety of orientations, in or out of a gravity field, without the need of an auxiliary power source for fluid pumping and without any moving parts.

The heat transport capability of a heat pipe may be limited by several effects [1]. At low temperatures viscous forces in the vapor flow are dominant. A condition may arise, called the viscous limit, where the pressure drop in the vapor is equal to the total vapor pressure in the heat pipe. The result is no vapor flow and, thus, no heat transfer. Conversely, a sonic limit occurs when inertial forces in the vapor flow are dominant and

TABLE 2.1. Various Heat Pipe Working Fluids

Medium	Melting point (°C)	Boiling point at atmos. press. (°C)	Useful range (°C)
Helium	- 272	- 269	- 271 - - 269
Nitrogen	- 210	- 196	- 203 - - 160
Ammonia	- 78	- 33	- 60 - 100
Freon 11	- 111	24	- 40 - 120
Pentane	- 130	28	- 20 - 120
Freon 113	- 35	48	- 10 - 100
Acetone	- 95	57	0 - 120
Methanol	- 98	64	10 - 130
Ethanol	- 112	78	0 - 130
Heptane	- 90	98	0 - 150
Water	0	100	30 - 200
Toluene	- 95	110	50 - 200
Mercury	- 39	361	250 - 650
Cesium	29	670	450 - 900
Potassium	62	774	500 - 1000
Sodium	98	892	600 - 1200
Lithium	179	1340	1000 - 1800

the vapor leaves the evaporator at a sonic speed. The vapor flow is "choked" and the maximum heat transfer rate is therefore limited. Both of these effects are typically important during the heat pipe startup. When the relative velocity between the liquid flow in the capillary structure and the vapor flow is large, the liquid-vapor interface may become unstable and liquid may be entrained in the vapor stream. Heat transfer is thus limited by this entrainment limit due to the loss of liquid from the capillary structure which never reaches the evaporator section. A capillary limit may be reached when the maximum capillary head is less than the total liquid and vapor pressure losses in the capillary structure. Finally, a boiling limit may occur when vapor production in the evaporator section impedes the return of liquid from the condenser section.

The heat pipe has been described and analyzed in numerous publications. The term "heat pipe" first appeared in 1963 in a patent application by Grover [2]. Shortly afterwards, researchers at the Los Alamos National Laboratory published the first technical paper describing the basic heat pipe operation [3]. The general theory for quantitatively predicting steady state heat pipe behavior was developed by Cotter [4].

Sun and Tien [5] conducted both theoretical and experimental studies of the performance of steady state heat pipes. Their analyses were performed using a single component conduction model with uniform vapor temperature and uniform injection into the vapor region.

Chang and Colwell [6] conducted a study of the transient characteristics of low temperature heat pipes numerically and experimentally. Their study assumed conduction

was the dominant mode of heat transfer through the heat pipe shell and wick, the thermal resistance between the wick and the vapor region was negligible, and the vapor temperature was only a function of time.

Hypersonic Leading Edge Cooling Using Heat Pipes

An initial consideration for using heat pipes as a means of cooling hypersonic vehicle leading edges was done by Silverstein [7]. In his theoretical cooling concept a continuous, isothermal heat pipe structure covered a vehicle wing leading edge, a portion of the lower wing surface, and a portion of the upper wing surface. Aerodynamic heating was absorbed at the leading edge and lower wing surface and transported through the heat pipe structure to the upper wing surface. There the energy was dissipated by means of radiation and convection. As a result of the parametric study, Silverstein concluded that heat pipe cooling was a feasible technique for limiting maximum leading edge temperatures of hypersonic vehicles.

Encouraged by this outcome, subsequent researchers conducted further analytical and experimental studies to investigate the feasibility of cooling hypersonic vehicle stagnation regions using heat pipes. Engineers from the McDonnell Douglas Astronautics Company and the NASA Marshall Space Flight Center [8] compared and evaluated a heat pipe cooled space shuttle wing leading edge against three alternate leading edge surface cooling/protection candidates: a refurbishable ablative design, a reusable columbium leading edge, and a reusable carbon-carbon leading edge. Each concept was shown to

be feasible. The ablative concept, however, was considered impractical because of its excessive cost (over three times that of the other concepts) and its potential adverse aerodynamic effects due to the changing wing leading edge geometry and surface roughness resulting from the ablative process.

Camarda [9,10] investigated the performance of a heat pipe cooled leading edge both experimentally and analytically. He conducted radiant heating tests and aerothermal load tests on a sodium filled, Hastelloy X heat pipe cooled leading edge model. His experimental results were in good agreement with previous analytical conclusions. His tests provided the first experimentally verified indication that liquid metal heat pipe cooling of hypersonic vehicle wing leading edges was feasible for lowering stagnation temperatures sufficiently enough to allow the use of available and durable superalloys.

Colwell, et al., [11] studied in detail the internal dynamics of liquid metal heat pipe operation. Particular emphasis was placed on examining the transient physical processes involved during heat pipe startup from a frozen state. Their work resulted in a more accurate mathematical model of transient heat pipe behavior under simulated space shuttle wing leading edge conditions.

Jang [12] further demonstrated the effectiveness of heat pipes in reducing peak temperatures in the vicinity of a space shuttle wing leading edge. His detailed work continued to support the feasibility concept of heat pipe cooling of hypersonic vehicle stagnation regions.

Colwell [13] has also demonstrated that heat pipe cooling alone was theoretically

sufficient to maintain a wing leading edge surface temperature below a design value of 1500 K during a typical re-entry mission of a National Aerospace Plane-type vehicle. However, he further indicated that for a typical ascent mission heat pipe cooling alone was not sufficient. It appeared that for a 50 minute ascent mission using heat pipe cooling, the maximum wing leading edge surface temperatures would exceed 1500 K for approximately 25 minutes. Thus, his work identified the requirement for additional cooling, along with heat pipe cooling, during this critical portion of an ascent mission of a National Aerospace Plane-type hypersonic vehicle.

Hendrix [14] studied analytically the effects of body forces, including gravity, on heat pipe performance in an aerospace plane-type wing leading edge. He found that these forces may affect the boiling and entrainment heat transfer limits of the heat pipe.

Glass and Camarda [15] conducted a preliminary design study of a carbon-carbon/refractory metal heat pipe aerospace plane wing leading edge. Their concept used a carbon-carbon primary structure with refractory metal heat pipes. External wing radiative cooling was supplemented by internal radiative cooling to a circulated hydrogen coolant heat exchanger. They found that during ascent heat pipe cooling supplemented with internal radiative cooling may be sufficient to produce a feasible design at peak heat fluxes. During descent their results showed that no supplementary cooling was required.

Alternative liquid metal heat pipe hypersonic flight applications have been investigated by Silverstein [16,17]. He has analyzed several heat pipe cooling concepts for SCRAMJET combustor liners and the use of a heat pipe cooling system which

employs a sensible heat sink.

Thus, the theme which underscores the reports in the literature is the consensus on the feasible use of liquid metal heat pipes to aid in cooling hypersonic vehicle leading edge regions. However, this concept is a relatively new application of heat pipe technology and has never been successfully field tested. What have successfully been tested under hypersonic flight conditions are the surface mass transfer cooling techniques: ablation, film cooling, and transpiration cooling.

Hypersonic Surface Mass Transfer Cooling

In the literature, the use of these surface cooling methods for missiles and reentry vehicles is well documented [18-28]. As shown in Figure 2.2, ablation cooling refers to the well controlled, uniform process of heat absorption and subsequent removal of surface material utilizing the material's thermal capacity for cooling [29]. Film cooling refers to the injection of a "cool" fluid into a "hot" boundary layer in such a manner that it forms a thin protective layer over the surface to be cooled. The fluid is injected at one or more discrete locations on the surface through holes or slots. Transpiration cooling refers to the injection of a coolant fluid through a porous surface into the hot boundary layer. In both film and transpiration cooling the protective effect of the heat absorption is augmented by the heat transfer blocking action of the coolant as it moves into the boundary layer. In effect, the presence of the coolant on the surface reduces the boundary layer velocity and temperature gradients at the hot surface thereby decreasing

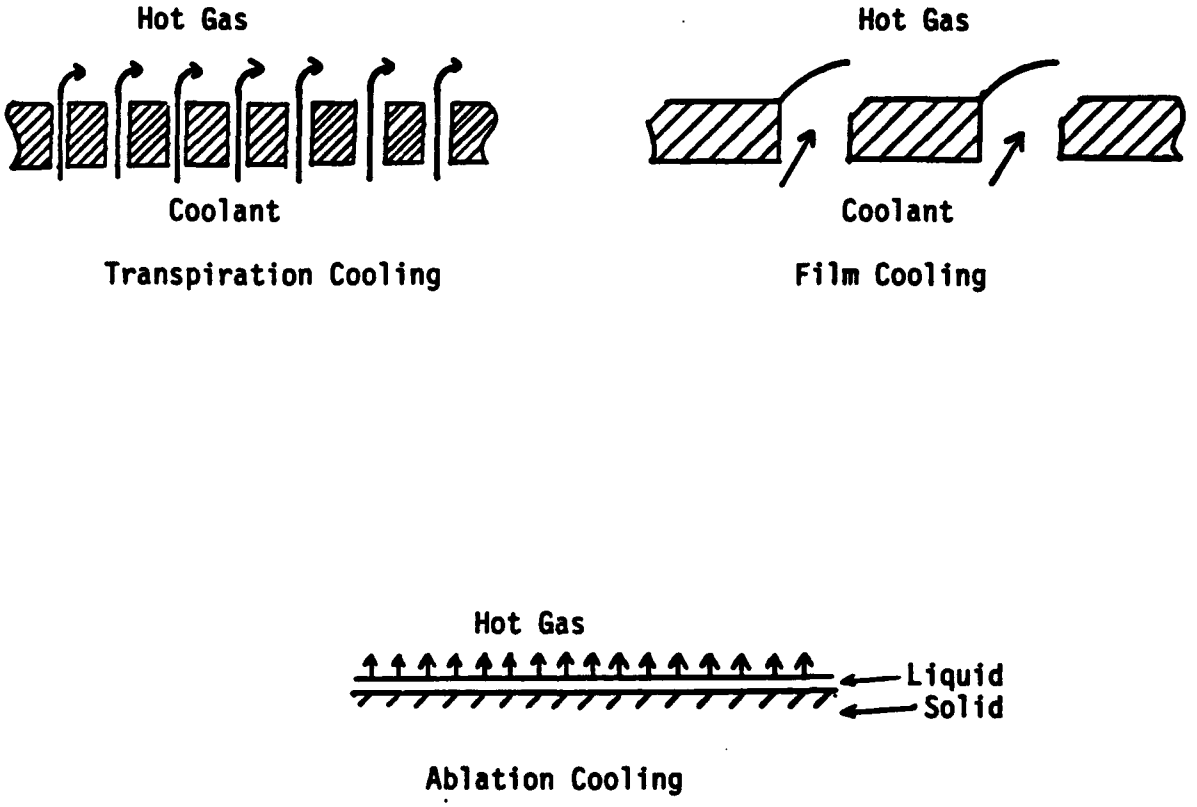

FIGURE 2.2. Various Mass Transfer Surface Cooling Techniques

the heat transfer rate to the surface [22].

For utilization as a potential cooling candidate in hypersonic aerospace plane-type vehicles, ablative cooling has lost favor over the other two surface mass transfer cooling methods for the reasons cited previously. Although the ablative material refurbishment problem is perhaps unavoidable, Camberos and Roberts [30] have recently proposed a possible solution to the changing leading edge geometry problem associated with ablation cooling. Their concept, involving a combination of radiation, ablation, and transpiration cooling, was to place an ablating material behind a fixed-shape, porous outer shield. During periods of excessive heating ablation occurs and the gaseous ablation products transpire through the outer shield. Their simplified, one-dimensional analysis corresponding to a typical glide re-entry trajectory indicated that ablative materials with thermal properties similar to teflon met the criteria necessary for a successful application of their method.

Other investigators have studied various aspects of the complicated and detailed heat transfer and fluid flow phenomena associated with mass addition into hypersonic laminar and turbulent boundary layers [31-73]. Reported results have generally been based on known isothermal or adiabatic surface conditions, on computationally intensive numerical solutions of the boundary layer equations modified to account for surface mass addition effects, and on generalized surface geometries (such as flat plates and cylinders). Besides that of Camberos and Roberts [30], very little additional work has been reported in the literature on using these cooling methods for the hypersonic aerospace plane

leading edge application.

McConarty and Anthony [74] conducted an analytical study of active cooling systems for wings of a Mach 6 cruise aircraft for NASA. The wing geometry analyzed closely resembled that of the space shuttle. They examined external surface transpiration and film cooling and internal surface spray and convective cooling. Their results indicated that transpiration and convective cooling were feasible alternatives for cooling the wing structure. Film cooling was not reliably evaluated due to insufficient hypersonic film cooling theory available to them at the time.

Tavella and Roberts [75] conducted a preliminary numerical study of air transpiration cooling applied to a NASA hypersonic all-body configuration flying at an altitude of 30,500 meters and a Mach number of 10.3. Their steady state analysis assumed that the aerodynamic heating at a particular location on the aircraft skin was balanced by heat radiated outward by the skin and heat convected away by the coolant. Heat conduction into the skin was not considered. Their results indicated that the necessary coolant mass flow rate required to maintain the skin radiation balance was approximately a local function of surface location and the feasibility of the cooling concept depended on the allowable skin temperature.

Consequently, to date there exists some information reported in the literature on the feasibility of using liquid metal heat pipe cooling and very little information available on using surface mass transfer cooling techniques to aid in protecting aerospace plane leading edge surfaces from the severe hypersonic aerodynamic heating environment.

Another alternative, in which there is presently no reported work, is to investigate the surface cooling feasibility of a combined liquid metal heat pipe/surface mass transfer cooling system.

CHAPTER III

HYPERSONIC LEADING EDGE COOLING MODEL

The work that has been done on applying liquid metal heat pipe cooling techniques to the problem of cooling hypersonic aerospace plane-type leading edges was discussed in Chapter II. Very little has been reported in the literature on using surface mass transfer cooling techniques for this problem and no work has been reported to date on incorporating both transient heat pipe cooling with surface transpiration or film cooling. This chapter discusses the general models that were used in the present study to develop a transient hypersonic vehicle leading edge cooling model that incorporates liquid metal heat pipe and surface mass transfer cooling. The complete description of the leading edge cooling model with applications to a leading edge are the topics of Chapters IV and V.

Numerical Heat Pipe Models

Figure 3.1 shows a schematic of a heat pipe cooled hypersonic leading edge with an active internal heat exchanger. Aerodynamic heating would occur on the outer skin.

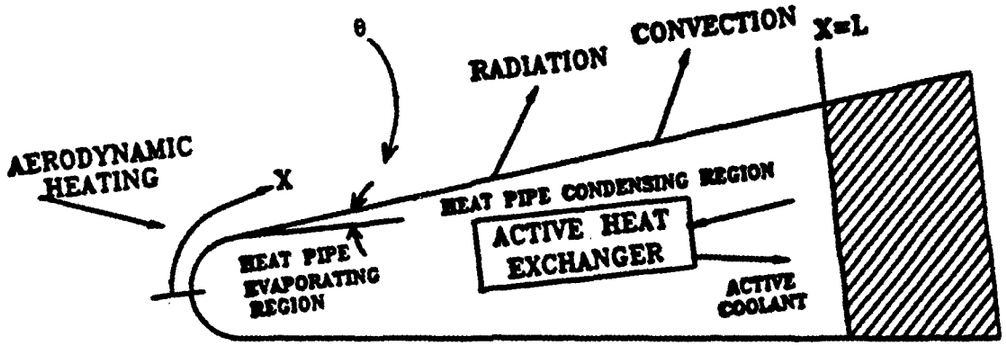

FIGURE 3.1. Schematic of a Heat Pipe Cooled Leading Edge with an Active Internal Heat Exchanger

Some of this energy would be conducted through the skin and into the working fluid vapor interior of the heat pipe in the evaporator section and some would be directly radiated away. Of the portion of energy conducted into the evaporator section, some heat may be taken away by the active heat exchanger. The remainder would be transferred through the heat pipe interior to the condensing region, conducted to the outer skin surface, and radiated away. The portion of the heat pipe which acts as the evaporator section would change as the aerodynamic heating and active heat exchanger coolant flow are changed. In general, for situations of very intense heating, such as in the case of aerospace plane leading edges, a significant active heat exchanger coolant flow could be required to aid in maintaining surface skin temperatures below a maximum acceptable level. Also under these conditions a large portion of the heat pipe capillary structure could operate in an evaporative mode with working fluid condensation occurring on the active heat exchanger surface. Working fluid return to the evaporator section would then have to be accomplished through additional capillary action or by other means. This could potentially complicate the leading edge design, the active internal heat exchanger design, or the overall cooling system performance. Additionally, for most vehicle flight conditions of interest heat fluxes and temperatures throughout the leading edge structure will vary with time. This results in some transient thermal response by the various masses within the structure.

Two numerical models have been developed for predicting transient aerodynamic heating effects on a heat pipe cooled leading edge and have been used as a basis for the

present work.

Finite Difference Model

A model which incorporated aerodynamic surface heating that varied with time and chordwise position, radiation or convection heat exchange with the surroundings, an active internal heat exchanger with a time varying heat load, and thermal properties that are temperature dependent has been developed. The model was originally formulated to simulate the transient operation of a rectangular heat pipe at low temperatures [6]. However, it has since been modified to predict the thermal performance of a leading edge heat pipe [13,14].

The model was based upon several assumptions. First, it was assumed that heat transfer through the heat pipe skin and capillary structure was by conduction only. This appeared to be a reasonable assumption and allowed for the use of a transient conduction equation to describe this effect.

Second, it was assumed there were negligible thermal resistances at the heat pipe liquid/vapor interface in the evaporator and condenser sections and within the vapor region itself. It has been shown experimentally that this assumption is reasonable for normal operating conditions of a leading edge heat pipe [9]. However, this assumption does not hold during startup conditions, that is, when the working fluid is being melted and vaporized. Thus, it was further assumed that there were no startup effects, that is, the working fluid was always operating in a continuum flow regime.

Fourth, spanwise temperature gradients along the leading edge were neglected. The

heat transfer was considered two-dimensional: conduction through and along the heat pipe shell and capillary structure. Since the entire vehicle leading edge would conceptually contain multiple heat pipes adjacent to one another separated only by a thin wing rib, this assumption seemed reasonable. Therefore, it was additionally assumed that the spanwise boundaries of the interior heat pipes were adiabatic, wing tip end effects were not considered, and the influence of the thin wing rib mass during transient periods was assumed negligible.

Lastly, the temperature distribution of the leading edge was assumed to be symmetric about the stagnation point. Thus, the stagnation line was considered adiabatic and heat transfer for the heat pipe could be evaluated using either the upper or lower leading edge surface. This assumption is actually only completely valid for symmetrically shaped leading edges flying at a zero angle of attack. However, the error caused by this assumption for non-symmetric leading edges and non-zero angle of attacks was not considered significant since curvature effects do not greatly affect heat pipe heat transfer performance [14]. Consequently, surface curvature was also neglected in this model.

Therefore, referring to Figure 3.2, the various heat pipe regions were mathematically described as:

Skin Conduction

$$\frac{\partial(\rho_1 C_1 T_1)}{\partial t} = \nabla\cdot[\kappa_1 \nabla T_1] \qquad (1)$$

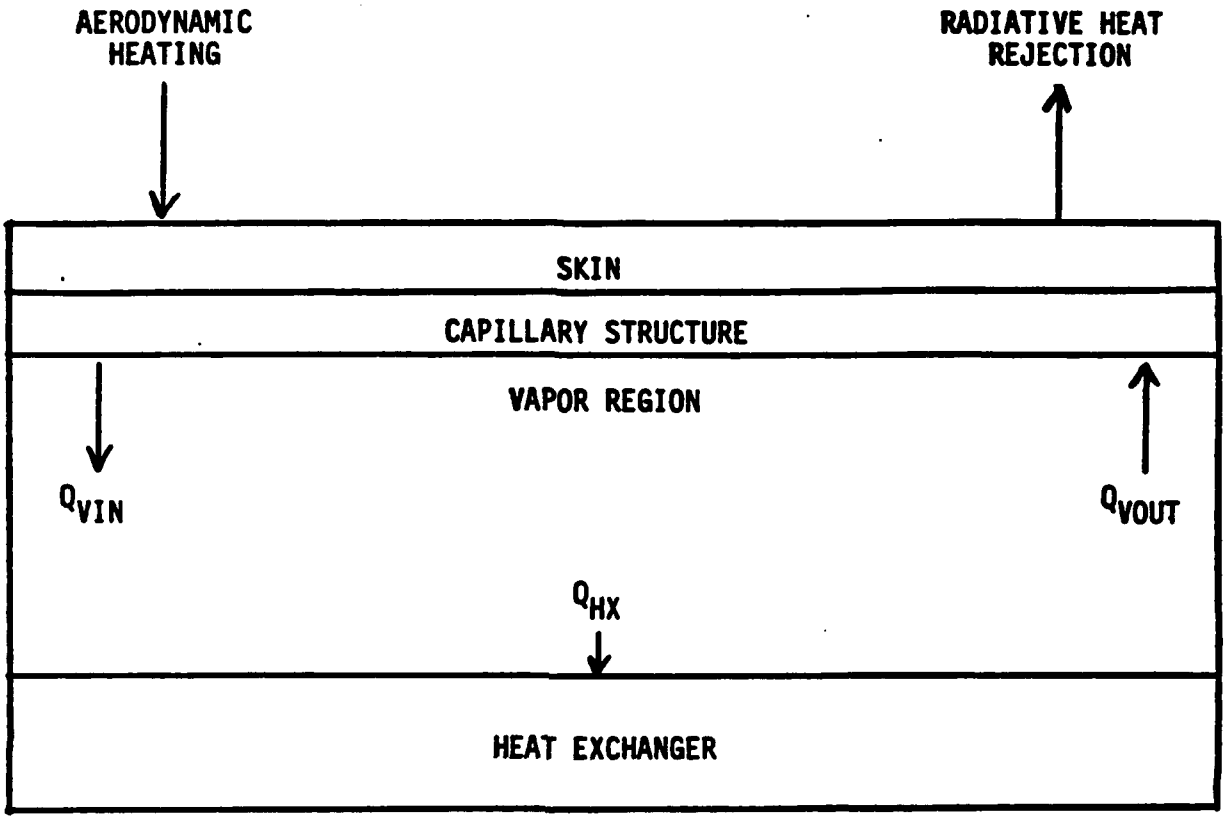

FIGURE 3.2. Schematic of the Heat Pipe Cooling Model Energy Balance

where $T_1 = T_1(x,y,t)$.

Capillary Structure

$$\frac{\partial(\rho_2 C_2 T_2)}{\partial t} = \nabla\cdot[\kappa_2 \nabla T_2] \tag{2}$$

where $T_2 = T_2(x,y,t)$ and properties were effective properties which accounted for working fluid properties, capillary structure properties, porosity, and temperature.

Vapor Region

$$-L \int_0^1 \kappa_2 \frac{\partial T_2}{\partial y}\Big|_V d(\frac{x}{L}) = Q_{HX} + \frac{1}{L}\frac{\partial(m_{HX} C_{HX} T_V)}{\partial t} \tag{3}$$

where $T_v = T_v(t)$.

Outer Surface

$$Q_{AERO} - Q_{RAD} + L \int_0^1 \kappa_1 \frac{\partial T_1}{\partial y}\Big|_{os} d(\frac{x}{L}) = 0 \tag{4}$$

where,

$$Q_{AERO} = L\, q_{STAG} \int_0^1 \frac{q}{q_{STAG}}\, d(\frac{x}{L}) \qquad (5)$$

$$Q_{RAD} = L \int_0^1 \epsilon\, \sigma\, (T_{1,os}^4 - T_\infty^4)\, d(\frac{x}{L}) \qquad (6)$$

and emissivity and absorptivity of the wing outer surface were assumed to be equal.

Skin/Capillary Structure Interface

$$-\kappa_1 \frac{\partial T_1}{\partial y}\Big|_{scs,x} = -\kappa_2 \frac{\partial T_2}{\partial y}\Big|_{scs,x} \qquad (7)$$

Based upon these governing equations, finite difference equations, logic schemes, and computer programs have been developed which predict the thermal behavior of a heat pipe cooled leading edge. This development was initially formulated based on a cylindrical geometry by Priester [76]. The model was further developed by Chang [77] and converted to a rectangular form by Hughes [78]. The numerical technique known as the alternating-direction-implicit method was used to write the transient finite difference equations. Details related to the formulation of these equations are discussed by Hendrix [14].

Hendrix checked the performance of this model by comparing its calculated

numerical results with transient experimental results of Camarda [9] for a fully started, space shuttle-type leading edge. He showed that there was generally good agreement between the calculated numerical and reported experimental results [14]. The predicted surface and vapor temperatures were between 50 K and 60 K greater than the measured values along the entire heat pipe length. However, it was felt that this temperature difference was due to the neglect of natural convection and other heat losses in the numerical calculations and the uncertainty of the surface emissivity used in the experimental results.

As evidenced by the model assumptions, this finite difference heat pipe model did not contain any expressions to describe the melting of the liquid metal working fluid in the capillary structure or the flow dynamics in the vapor space. These considerations are typically important during the initial phase of an ascent mission for the aerospace plane. During this phase the heat pipe would be at ambient temperature with the working fluid in a frozen state and free molecular flow in the vapor space. Thus, without adequate expressions to model these phenomena the finite difference numerical model was only considered reliable to predict fully started, transient and steady heat pipe behavior.

Finite Element Model

A finite element numerical model has also been developed to predict the transient thermal performance of a liquid metal heat pipe [12]. This model was similar to the finite difference model developed earlier except that it did account for the working fluid melting phenomena during startup and the vapor dynamics associated with transition from

free molecular to continuum flow. After heat pipe startup, it was shown that both this model's and the finite difference model's numerical results compared well with each other and experimental measurements [13,79]. However, as expected they differed greatly at intermediate times during the heat pipe startup [80]. These differences occurred due to working fluid melting, transition from free molecular to continuum flow, and choking conditions which were only included in the finite element model. Additionally, a small amount of difference was attributed to curvature effects which were only included in the finite element model.

Surface Mass Transfer Cooling Models

As discussed earlier, numerous researchers have investigated the detailed heat transfer and fluid flow phenomena associated with surface mass transfer cooling. The result of these studies yielded an equally numerous amount of theoretically, empirically, and numerically based expressions for describing these phenomena for a variety of heating, flow, and surface conditions. The hypersonic aerospace plane heat pipe cooled leading edge application studied in the present investigation, on the other hand, did not precisely match the operating conditions assumed for the relationships previously developed in the literature. Furthermore, the interest in the present study was on the heat pipe cooled hypersonic leading edge structural response to aerodynamic heating/surface mass transfer cooling effects, not on the detailed boundary layer or flow-field response to coolant mass injection. Thus, due to this interest and the lack of

applicable experimental results, it was desired to model the transient surface mass transfer cooling effects in the present investigation with generalized expressions derived from the literature that approximated well the more exact theoretical predictions and experimental results from which they were based. It was envisioned, then, that the resulting generalized cooling model would be of value for: 1) assessing the feasibility of cooling hypersonic aircraft leading edges using liquid metal heat pipes with supplementary surface mass transfer cooling and, 2) for subsequent, more detailed engineering design calculations. This philosophy was used in identifying the following transpiration and film cooling models to be used with the finite difference heat pipe model to form the hypersonic leading edge cooling model.

Transpiration Cooling Model

Gross, et al., [60] developed generalized expressions for predicting skin friction and heat transfer in the presence of transpiration cooling for laminar flow over a surface with zero pressure gradient. This work was a result of an analysis initiated to present correction factors which must be applied to solid-wall calculations (in the absence of transpiration cooling) to account for the skin friction and heat transfer reduction effects of mass addition into a laminar boundary layer. It was found that by normalizing the experimental results of work done by previous investigators, the results correlated well with a dimensionless mass transfer parameter. For heat transfer reduction the following expression was developed:

$$\frac{q}{q_0} = 1 - 1.82 \left(\frac{M_{AIR}}{M_{COOL}}\right)^{1/3} \left(\frac{\rho_w v_w}{\rho_e \mu_e}\right) \left(\frac{Re_x}{C^*}\right)^{1/2} \quad (8)$$

where Re_x was based on boundary layer edge conditions,

$$C^* = \frac{\rho^* \mu^*}{\rho_e \mu_e} \quad (9)$$

and $\rho^* \mu^*$ were evaluated at the Eckert [62] reference temperature, T^*, which can be expressed, as suggested by Laganelli [37], by:

$$T^* = T_e + 0.72 (T_r - T_e) \ . \quad (10)$$

The correlating dimensionless mass transfer parameter was the term:

$$J = \left(\frac{\rho_w v_w}{\rho_e \mu_e}\right) \left(\frac{Re_x}{C^*}\right)^{1/2} \ . \quad (11)$$

Limitations of the laminar, flat plate, transpiration cooling correlation, Equation (8), were two-fold. First, Gross, et al., [60] indicated that the correlation was generally valid for the dimensionless mass transfer parameter, J, having an upper bound of 0.25 to 0.3, or:

$$I \rho_e \left(\frac{u_e}{(\rho \mu)^*}\right)^{1/2} x^{1/2} \leq 0.25 \ . \qquad (12)$$

where,

$$I = \frac{\rho_w v_w}{\rho_e u_e} \qquad (13)$$

and Equation (9) was substituted into (11) and simplified.

The second limitation resulted from the velocity boundary layer thickening due to mass addition. Excessive transpiration could lead to destabilization of the laminar boundary layer. For air injection it was reported that this can occur when:

$$K = I (Re_x)^{1/2} \geq 0.619 \qquad (14)$$

while lighter gases tended to be more destabilizing [60].

Also addressed by Gross, et al., [60] was the effect of pressure gradient on laminar mass transfer cooling. The greatest heat transfer reduction occurred for the zero pressure gradient condition (flat plate flow) and the least reduction for plane stagnation flow. However, for values of the dimensionless mass transfer parameter, J, less than 0.1 the difference in heat transfer reduction between the flat plate condition and plane stagnation

flow condition was small.

Film Cooling Model

As discussed in the previous section, the desire in the present study was to represent the transpiration and film cooling effects in terms of a heat transfer reduction correlation. Unfortunately, in the literature almost all reported work in film cooling presented results in terms of a film cooling effectiveness parameter rather than a surface heat transfer reduction due to film cooling. The effectiveness parameter, although defined in various ways by different researchers, was generally expressed as a ratio of temperature differences in the form of:

$$\varepsilon_{film} = \frac{T_{w,film} - T_{\infty}}{T_{w,o} - T_{\infty}} \quad . \tag{15}$$

Presenting film cooling results in terms of an effectiveness parameter was primarily derived from turbulent film theory and experimental verification. This was due to the inherent difficulty of maintaining a laminar film over a surface in an experimental setup. However, for the present application it was expected that a laminar boundary layer would cover most of the hypersonic surface's leading edge and it was desired to have a film cooling heat transfer reduction correlation for laminar flow, similar in form to Equations (4) and (8).

Redeker and Miller [23] have shown a good correlation between experimental and theoretical studies of laminar film cooling using a one inch nose radius hemi-cylinder

slab, approximating a full scale wing, in Mach 16 flow. Their theoretical film cooling development was based on a discrete layer flow model presented by Hatch and Papell [72]. Using a basic principles/control volume approach at the surface stagnation point, Redeker and Miller developed the following relationship for the heat transfer reduction due to laminar film cooling an isothermal, non-adiabatic surface:

$$\frac{q_{w,film}}{q_o} = \frac{A}{1+A}(1-e^{-B}) \tag{16}$$

where,

$$A = (\frac{M_{COOL}}{M_{AIR}})^{1/2}(\frac{Cp_{COOL}}{Cp_{AIR}}) \tag{17}$$

and,

$$B = \frac{2(1+A)}{(\frac{\dot{m}}{\ell}Cp)_{COOL}} \int_0^x h_a\,dx \quad . \tag{18}$$

Next, they then conducted a number of experiments designed to measure the heat transfer reduction due to laminar film cooling on the hemi-cylinder slab in Mach 16 flow. Coolants used were gaseous nitrogen and helium at several mass flowrates. Both surface

tangential to and normal to the stagnation line coolant injection methods were investigated.

Their results indicated that substantial reductions in aerodynamic surface heating could be obtained by film cooling. The tangential injection was shown to be more effective than normal injection. Additionally, they found a very good correlation existed between the experimental results and the predicted analytical results from Equation (16). To have this correlation, however, required knowledge of the functional relationship between the heat transfer coefficient, h_x, and surface distance, x. This heat transfer coefficient, based upon the temperature difference between the boundary layer air and the injected coolant film, was determined experimentally in their study.

For the application of interest in the present investigation this relationship was unknown. Additionally, the relationship between the boundary layer air-to-surface heat transfer coefficient and surface distance (the no coolant injection case) was unknown, along with the chordwise leading edge surface temperature distribution. These conditions all being due to the lack of available experimental data.

Consequently, it was felt that although Equations (8) and (16) provided the most reasonable, experimentally correlated, generalized heat transfer reduction relations available in the literature for laminar transpiration and film cooling, they needed further modification to be applicable to the hypersonic leading edge cooling problem of the present work. Chapters IV and V detail how these generalized transpiration and film cooling models were adapted and combined with the liquid metal heat pipe model to

develop a leading edge cooling model for hypersonic flow applications.

CHAPTER IV

COOLING MODEL APPLICATION : WING LEADING EDGE

The generalized models selected from the literature and considered for use in the present investigation of developing and analyzing a hypersonic leading edge cooling model which incorporates liquid metal heat pipe, transpiration, and film cooling were discussed in Chapter III. However, the transpiration and film cooling models reported in the literature were not directly applicable to the problem of interest in this study. Further modifications, assumptions and analysis were required in order to attain the goal of developing a workable leading edge cooling model and analyzing its application to hypersonic aerospace plane vehicle leading edges. This chapter details the procedure used to accomplish this goal.

Hypersonic Leading Edge Operational Characteristics

In order to completely formulate the leading edge cooling model some information on typical hypersonic leading edge operating conditions had to be assumed. Knowledge of these conditions allowed the determination of: the aerodynamic surface heating rate

distributions, a hypersonic flow-field analysis, the required thermodynamic and flow-field properties and the applicable modifications to the generalized transpiration and film cooling models.

Referring to Figure 3.1, it was initially assumed that the hypersonic leading edge of interest represented an aerospace plane wing section having a nose radius of 0.031 meter (0.5 inch), a sweep angle of 70 degrees, a wedge half-angle, θ, of 7 degrees, and a leading edge length of 0.4029 meter (16 inches). A lithium filled heat pipe spanned the entire leading edge length. The 0.0005 meter thick heat pipe shell was made of a columbium alloy and the molybdenum wick was 0.00076 meter thick. Its thermal properties are described by Hendrix [14] and Morrison [80]. The aircraft executed an approximately constant 2000 psf dynamic pressure ascent mission, following the flight trajectory shown in Figures 4.1 and 4.2, and thus remaining in a continuum flow regime.

The flow-field in the vicinity of the aerospace plane wing was modeled by assuming the presence of a detached bow shock upstream of the wing. Flow through the shock, in the vicinity of the leading edge, was modeled as flow through a normal shock. The air flow after the shock front was assumed to be in local thermo-chemical equilibrium. That is, the air flow was treated as a high temperature, chemically reacting, inviscid (except in the boundary layer), equilibrium flow. The air properties at the edge of the leading edge boundary layer were assumed to be equal to those immediately after the shock front. As a result of the large air density increase and velocity decrease typical of flow across a normal shock, the boundary layer flow over the entire 0.4029 meter

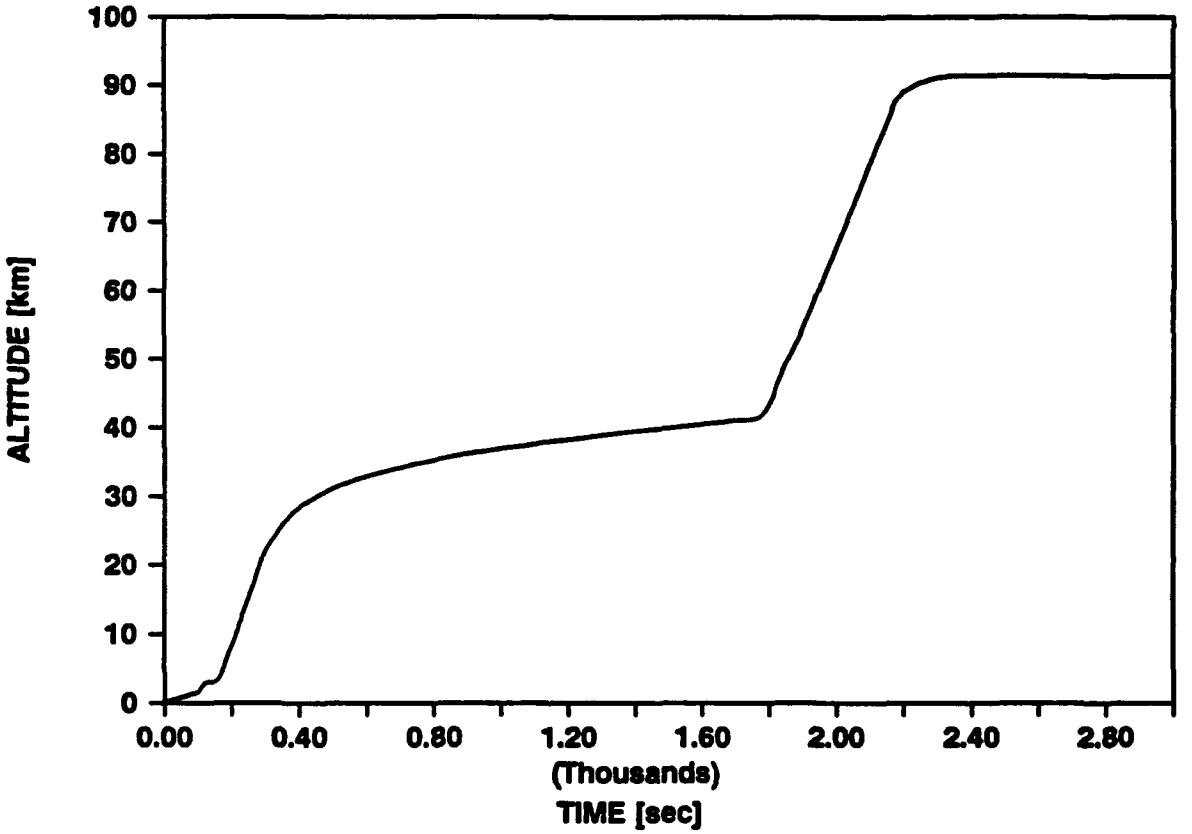

FIGURE 4.1. A Typical Hypersonic Vehicle Ascent Flight Trajectory

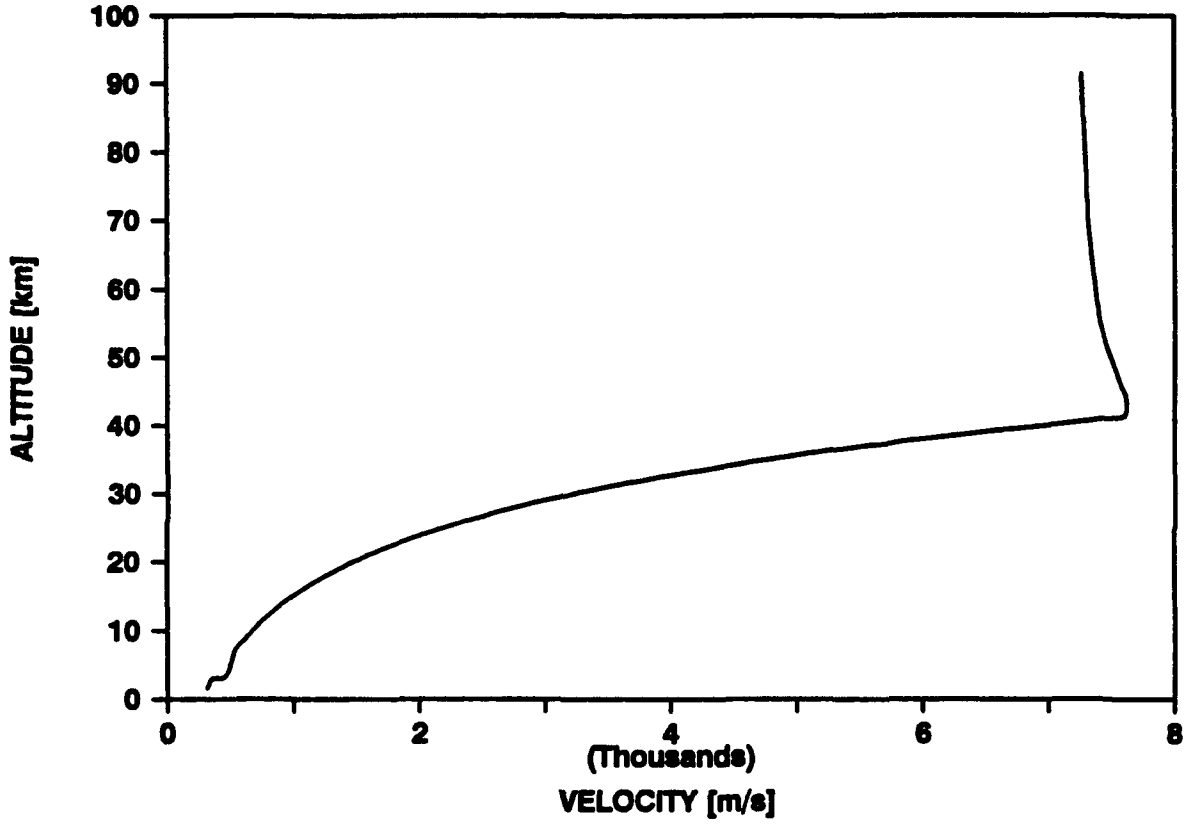

FIGURE 4.2. A Typical Hypersonic Vehicle Velocity-Altitude Map

leading edge was assumed to be laminar. Lastly, it was assumed there were neither shock-boundary layer interactions nor shock-shock interference effects present in the vicinity of the wing leading edge. This last assumption will be relaxed in the next chapter when SCRAMJET engine inlet leading edge cooling is discussed.

Transpiration and Film Cooling Model Modifications

Recall, the finite difference heat pipe model discussed in Chapter III was developed from an energy balance consideration. In order to additionally incorporate the effects of surface cooling due to transpiration and film cooling, it was advantageous to express the transpiration and film cooling relationships in terms of energy reduction parameters. This requirement is expressed by the form of Equations (8) and (16). Furthermore, the transpiration relationship, Equation (8), was based on a correlation of laminar, flat plate experimental data, while the film cooling expression, Equation (16), required additional information about the heat transfer coefficient, h_a. Both equations, therefore, needed further modifications and assumptions made in order to be applicable to the present leading edge study.

Transpiration Cooling

Equation (8) was developed to represent the general heat transfer reduction to a flat plate surface as a result of coolant transpiration into a laminar boundary layer. It was initially felt, for the purpose of the present investigation, that the air flow over the leading edge would be best represented as being somewhere between flat plate and plane

stagnation flow. However, Gross, et al., [60] demonstrated that the difference between the flat plate and plane stagnation flow heat transfer reduction was small for low values (less than 0.1) of the dimensionless mass transfer parameter, J, in Equation (11). Therefore, based on that result, on the assumed geometric shape of the wing leading edge (sharp nose radius versus leading edge length, small wedge angle), and on the negligible effect curvature has on heat pipe performance, the leading edge surface in the present study was modeled as a flat plate for transpiration cooling while ensuring that values of J, near the stagnation point, remained less than 0.1.

Equation (8) may also be expressed in terms of a dimensionless length parameter, x/L, where L equals the applicable leading edge length, using Equations (9), (13) and the definition of Re_x as:

$$\frac{q_{AERO}}{q_{SP}} = 1 - 1.16 \left(\frac{M_{AIR}}{M_{COOL}}\right)^{1/3} I \, \rho_e \left(\frac{u_e}{(\rho \mu)^*}\right)^{1/2} \left(\frac{x}{L}\right)^{1/2} \qquad (19)$$

Film Cooling

In order to evaluate Equation (18) for use in the film cooling reduction expression, Equation (16), additional information was required on the functional relationship between h_a and x. Since this data is only available experimentally, it was first assumed in this study that the boundary layer-to-coolant film heat transfer coefficient, h_a, was equal to the boundary layer-to-leading edge surface heat transfer coefficient, h, as suggested by Swenson [61]. Second, it was assumed that the Reynolds analogy for flow over a flat

plate was valid for this application, that is:

$$St\ Pr^{2/3} = \frac{c_f}{2} . \tag{20}$$

Although developed from an incompressible flat plate flow analysis, it has been shown that the Reynolds analogy relating fluid friction and heat transfer gives reasonable approximations at hypersonic speeds and that this trend also holds for hypersonic boundary layers over general aerodynamic shapes [81].

Therefore, from the definition of the Stanton number and the above assumptions, h_a can be expressed as:

$$h_a = h = St(\rho\ Cp\ u)_e \tag{21}$$

where all air properties are evaluated at the boundary layer edge. Employing the analogy yields:

$$h = .332\ Re_x^{-1/2}\ Pr^{-2/3}(\rho\ Cp\ u)_e . \tag{22}$$

Integration of Equation (22) results in:

$$\int_0^x h\,dx = .664\ Pr^{-2/3}\ Cp\ (\rho\,\mu\,u\,x)^{1/2}\ . \qquad (23)$$

Further, to better approximate a compressible flow condition by an effective incompressible one, Equation (23) can be modified, as suggested by Laganelli [37], by using:

$$h^* = \left(\frac{\rho^*}{\rho_e}\right) h \qquad (24)$$

where $(\ )^*$ air properties are evaluated using the reference temperature, Equation (10). Incorporating this modification into the integration of Equation (22) yields:

$$\int_0^x h^*\,dx = .664\ Pr^{*\,-2/3}\ Cp_e\ (\rho\,\mu)^{*\,1/2}\ u_e^{1/2}\ x^{1/2} \qquad (25)$$

where the variation of Pr with Pr^* was considered small.

Using Equation (25), Equation (18) can be rewritten as:

$$B = 1.68\ \frac{(1+A)}{\dot{w}_{COOL}}\left(\frac{Cp_e}{Cp_{COOL}}\right)(u_e(\rho\,\mu)^*)^{1/2}\ x^{1/2} \qquad (26)$$

for $Pr^* = 0.71$ and:

$$\dot{w}_{COOL} = \left(\frac{\dot{m}}{\ell}\right)_{COOL} . \qquad (27)$$

To check the validity of using Equations (16), (17), and (26) for the film cooling model of this work, their numerically predicted heat transfer reduction results were compared with the corresponding experimentally determined results reported by Redeker and Miller [23] for nitrogen at various x locations along their test surface and values of coolant mass flowrate per unit span length. The result of this comparison is shown in Table 4.1. It appears that the approximations discussed above slightly overpredict the experimental results at higher values of coolant mass flowrate per unit span length and underpredict them at lower values. At the lower values of coolant mass flowrate per unit span length, the approximations appear to predict a relatively constant heat transfer reduction with distance. This is not entirely consistent with film cooling theory [72], but tends to follow the same trend as the reported experimental data. Since the predicted values of heat transfer reduction are based on Equation (16), the reduction should, theoretically, decline somewhat exponentially because of the $(1 - e^{-B})$ term. As seen in Equation (26), the parameter B is proportional to $x^{1/2}$ and inversely proportional to coolant mass flowrate per unit span length, $\dot{w}_{COOL}$. It appears, then, in the case of very low coolant mass flowrates per unit span length the parameter B becomes excessively large, the $(1 - e^{-B})$ term approaches 1, and the heat transfer reduction is governed by the term $A/(1+A)$. Thus, this approximation seems to work best at higher values of $\dot{w}_{COOL}$.

TABLE 4.1. A Comparison of the Experimental Results of Redeker and Miller [23] to the Numerical Results of Equation (16)

x[m]	$\dot{w}_{COOL}$=0.66		$\dot{w}_{COOL}$=0.26		$\dot{w}_{COOL}$=0.03		$\dot{w}_{COOL}$=0.02	
	REF [23]	EQN (16)	REF [23]	EQN (16)	REF [23]	EQN (16)	REF [23]	EQN (16)
0.01	0.15	0.21	0.2	0.30	0.4	0.34	0.55	0.34
0.02	0.2	0.24	0.3	0.32	0.5	0.34	0.6	0.34
0.06	0.2	0.30	0.3	0.34	0.5	0.34	0.5	0.34
0.18	0.2	0.33	0.4	0.34	0.5	0.34	0.6	0.34

Additionally, Redeker and Miller [23] reported no boundary layer transition to turbulence due to the coolant film injection at the flowrates used in their work. Therefore, to ensure good numerical approximations and a stable laminar boundary layer a value of coolant mass flowrate per unit span length greater than 0.1 and less than 0.3 was considered adequate for the present study.

As was done in the transpiration cooling case, for film cooling Equation (26) may be further expressed in terms of x/L by:

$$B = 1.07 \frac{(1+A)}{\dot{w}_{COOL}} \left(\frac{Cp_e}{Cp_{COOL}}\right) (u_e(\rho\mu)^*)^{1/2} \left(\frac{x}{L}\right)^{1/2} . \qquad (28)$$

Aerodynamic Heating Analysis

Equations (16), (17) and (28) for film cooling and Equation (19) for transpiration cooling express these surface cooling effects in terms of dimensionless heat transfer reductions heavily dependent upon the air properties at the boundary layer edge. Figures 4.1 and 4.2 imply that the hypersonic vehicle of interest to this study is exposed to a transient flight condition. Therefore, to incorporate these cooling models with the heat pipe leading edge cooling model, information about the transient hypersonic flow-field in the vicinity of the leading edge was required. This section discusses the aerodynamic heating analysis developed for the present study. The next section details the procedure used to determine the appropriate air properties.

Several investigators have examined the problem of aerodynamic heating of surfaces in hypersonic flow [54,55,59,62,66,82-96]. Based on the earlier theoretical work of others, Lees [54] conducted a classical analysis of laminar heat transfer over blunt-nosed bodies at hypersonic speeds. He developed relationships for surface heat transfer rate distributions for an isothermal hemispherical nose and a blunt cone. These relationships expressed the ratio of the local surface heat transfer rate to the maximum surface heat transfer rate at the stagnation point as a function of surface location. Applying these results to the particular hypersonic leading edge of the present study, allowed for the determination of the chordwise direction surface aerodynamic heat flux distribution shown in Figure 4.3. This distribution permitted the determination of the aerodynamic surface heating on the leading edge for the case of no coolant injection, q_o, in the heat transfer reduction equations developed earlier for transpiration and film cooling. However, in order to determine the aerodynamic heat input at a particular location along the leading edge surface, data also had to be developed on the transient nature of the stagnation point heat transfer rate.

Fay and Riddell [55] conducted a theoretical analysis of stagnation point heat transfer for high speed flight. Their results provided numerical solutions to the stagnation point boundary layer equations for both the thermo-chemical equilibrium and non-equilibrium cases. For the equilibrium case assumed in the present study, they determined that the stagnation point heat transfer rate was a strong function of: 1) the air flow properties (density, viscosity, enthalpy) at the boundary layer edge and at the surface stagnation

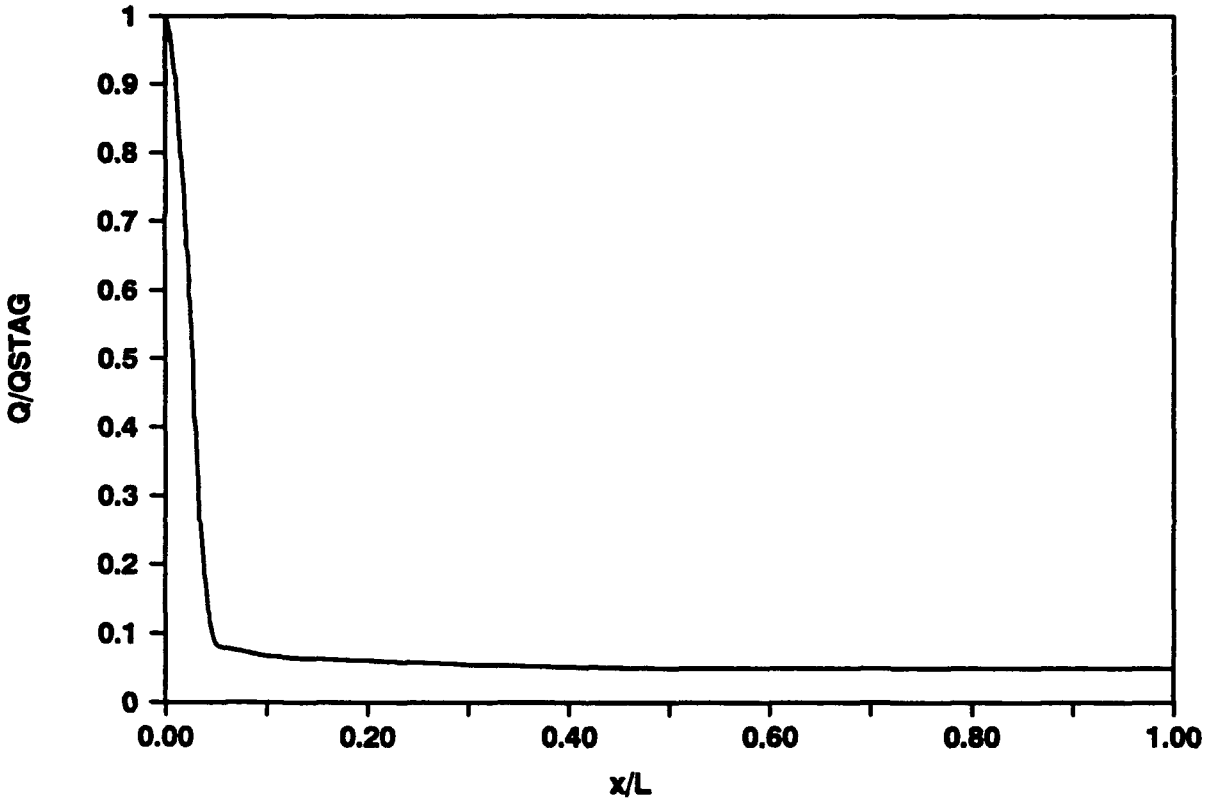

FIGURE 4.3. Aerodynamic Surface Heat Flux Distribution, Chordwise Direction

point, and 2) the boundary layer edge velocity gradient, in the flow direction, at the stagnation point. The difficulty of using this result in the present study included: the a priori determination of the stagnation point property values at the leading edge surface, the determination of the stagnation point velocity gradient, and the need to represent the aerodynamic heating as a function of time as well as location.

These blunt-body results can be used immediately for the heat transfer analysis of the nose of the aerospace plane. However, the high local heating occurring along the wing leading edge also depends upon the wing planform shape, the sweep angle, the leading edge nose radius, and the trajectory dynamic pressure. A relationship approximating the transient aerodynamic heating of a hypersonic leading edge, including these effects, has been developed and experimentally verified from space shuttle data by Tauber, et al., [94]. Based upon a swept-cylinder theory, their relationship applies in the flight regime where boundary layer theory is valid and appeared to yield good approximations for both laminar and turbulent boundary layer flow conditions in the absence of mass addition. The expression developed for the transient aerodynamic heating rate of a swept hypersonic leading edge, q_{AERO}, was:

$$q_{AERO} = [0.5(q_{SP})^2 \cos^2 \Delta + (q_{FP})^2 \sin^2 \Delta]^{1/2} \qquad (29)$$

where q_{SP} represented the unswept stagnation point heat flux, q_{FP} represented the heat flux along the flat plate portion of an unswept leading edge, and Δ represented the

leading edge sweep angle.

To determine the transient aerodynamic heating at the stagnation point for the swept leading edge of the present study, q_{FP} of Equation (29) was set equal to zero. Tauber, et al., [94] showed that for the hypersonic ascent of an unswept leading edge, q_{SP} could be approximated well by:

$$q_{SP} = 1.83(10^{-4})(2\wp)^{1/2}(r_n)^{-1/2}\left(1-\frac{h_w}{h_{SP}}\right)V_\infty^2 \qquad (30)$$

where q_{SP} was in [W/m^2], $\wp$ was the dynamic pressure in [Pa], r_n was the leading edge nose radius in [m], and V_∞ was the free-stream flight velocity in [m/sec]. Substituting Equation (30) into Equation (29) and setting q_{FP} equal to 0 allowed for the determination of the transient stagnation heat flux, QSTAG, profile for the swept leading edge of the present study. For the assumed flight conditions, the enthalpy term $(1-h_w/h_{SP})$ in Equation (30) was on the order of one and the air flow behaved as a continuum. Figure 4.4 shows the resultant transient aerodynamic stagnation heat flux used in this work.

High Temperature Air Analysis

As discussed earlier, the transpiration and film cooling models used in this investigation required information on the surrounding leading edge hypersonic flow-field. This section will present the assumptions and analysis used to determine the high temperature, inviscid, equilibrium air flow properties, in the vicinity of the leading edge,

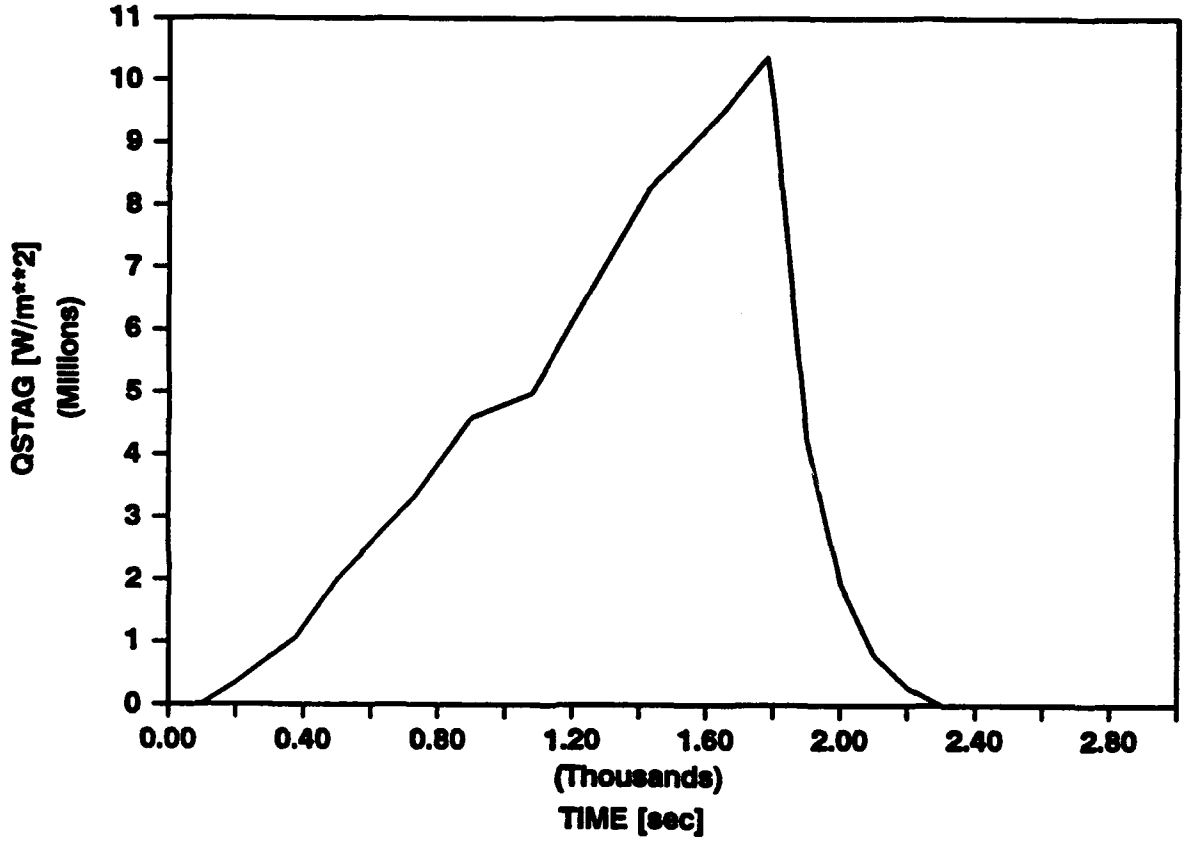

FIGURE 4.4. Transient Stagnation Aerodynamic Heat Flux

that were required for use in the surface cooling models and the aerodynamic heating relationships.

For the purpose of this study, it was assumed that the leading edge shock was strong enough, hence the air temperature after the shock was high enough, that vibrational excitation and chemical reactions occurred behind the shock front. As stated earlier, it was assumed that local thermodynamic and chemical equilibrium conditions held behind the shock. These assumptions were deemed necessary in this study due to the importance of high temperature air effects associated with hypersonic atmospheric flight. For lower speed flow it is generally an acceptable practice to treat air as an ideal gas, assume its specific heats are constant, its specific heat ratio equals 1.4 and that there are no vibrational excitation or chemical reaction concerns. However, it has been shown that this assumption considerably overpredicts the actual air temperature for Mach number flows greater than approximately 8 [96,98,99]. In an ideal gas assumption, the kinetic energy of the air flow ahead of the shock is primarily converted to translational and rotational energy behind the shock. On the other hand, by treating the air as a perfect gas (where Cp=Cp(T)) and/or a chemically reacting gas, the kinetic energy of the flow is also converted to additional molecular energy modes and/or the products of the chemical reactions behind the shock front. Thus, under these assumptions, the temperature of the air, which is essentially a measure of its translational energy only, is less and more closely predicts the actual temperature. Another effect of the high temperatures, which may cause a slight error in calculations, is the reduction in

magnitude of the specific heat ratio, γ. For air this ratio of Cp/Cv decreases from 1.4, at lower temperatures, to between 1.1 and 1.2 at higher temperatures associated with hypersonic flow [54].

The governing equations describing high temperature, inviscid, equilibrium flow are well established in the literature. Closed-form solutions to these equations, however, have not been obtained [81]. Thus, solutions to these flow problems have generally required extensive numerical computations and tabulation [88-90,97-99]. As an example, Huber [88] has given detailed results for equilibrium normal shock properties of high temperature air as a function of free-stream velocity and altitude. For this study, the results reported by Huber and Figures 4.1 and 4.2 were used to determine the air temperature and density after the wing leading edge shock front for the vehicle ascent mission. These properties were assumed to equal the air temperature and density at the edge of the leading edge surface boundary layer. Boundary layer edge velocity was determined from a continuity consideration by:

$$u_e = \frac{\rho_\infty u_\infty}{\rho_e} \quad . \tag{31}$$

Also at the boundary layer edge, viscosity effects became important. The kinematic viscosity at this location was determined using the power law relation suggested by Liepmann and Roshko [101]:

$$\frac{\mu_e}{\mu_\infty} = \left(\frac{T_e}{T_\infty}\right)^{\omega} \tag{32}$$

where ω=0.76 for air.

Finite Difference Computer Model

Having developed the appropriate expressions for laminar hypersonic leading edge surface transpiration and film cooling, determined the applicable thermodynamic and flow properties, and analyzed the transient, surface chordwise direction aerodynamic heat flux distribution, a finite difference based computational technique was formulated to provide the numerical development of the present study. As discussed in Chapter III, a finite difference computer model has been previously developed and verified with experimental data which predicts the transient surface and internal vapor temperatures of a liquid metal heat pipe cooled hypersonic leading edge. For the present study, this model required modification to allow for the additional effects of surface transpiration or film cooling.

The heat transfer reduction effects due to transpiration, Equation (19), and film cooling, Equations (16), (17), and (28), were incorporated as new boundary conditions into the computer model at a point where the aerodynamic surface heating calculations occur, Equation (5). Since the aerodynamic heat flux considered in this investigation was a function of both time and distance, data files to be read into the computer code were created listing the transient stagnation point heat flux values and the normalized,

chordwise surface heat flux distributions of Figures 4.3 and 4.4.

Again since q_{AERO}/q_{SP} varied with time and surface distance, the transpiration and film cooling expressions needed to vary similarly and data files were developed containing the transient values for the thermodynamic and flow properties indicated in those expressions. These properties were determined using the analysis discussed in the previous section. However, an assumed transient distribution for the dimensionless parameter, I, in Equation (19) had to be developed for three reasons. First, by examining Equation (13) the coolant mass flux into the boundary layer term, $(\rho_w v_w)$, had to be accounted for. Second, recall that Equation (12) represented a limitation to the applicability of the transpiration cooling model. Equation (12) indicates that the parameter, I, must not only be a function of time (since the air properties are transient) but must also be a function of surface distance, x. This seems reasonable since in an application of this cooling concept it would be appropriate to inject the surface coolant during the mission times when surface heating was most severe and to inject the most coolant at the surface locations nearest the stagnation region. Therefore, the transpiration coolant surface distribution used in this study was selected to match that used for the aerodynamic surface heating distribution. Third, the parameter, K, in expression (14) had to be less than 0.619 to ensure the laminar boundary layer remained stable during the coolant transpiration. Using these factors, the transpiration coolant transient distribution was determined and is shown in Figure 4.5. This data was also placed in a file for use by the computer model. Table 4.2 shows how the

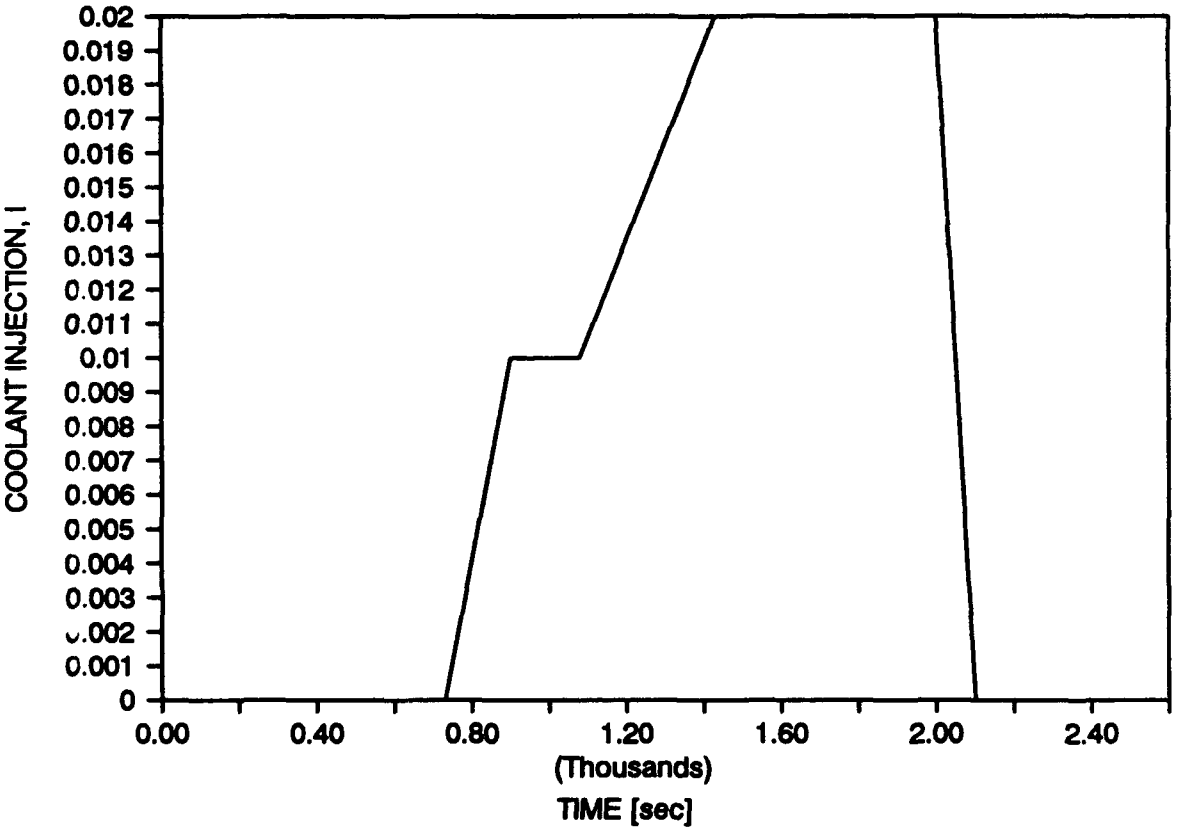

FIGURE 4.5. Transient Nondimensional Transpiration Coolant Injection Profile

TABLE 4.2. Values of the Nondimensional Parameters I, J, K and Re_x for Various Times and Surface Locations

Time[s]	x/L	I	J	K	Re_x
900	.0001	.01	.031	.031	10
	.001	.00995		.10	98
	.0125	.0087		.304	1219
	1.0	.0005		.156	9.75E+4
1430	.0001	.02	.049	.049	6
	.001	.0199		.155	61
	.0125	.0174		.48	762
	1.0	.001		.247	6.10E+4
1780	.0001	.02	.046	.046	5
	.OO1	.0199		.145	53
	.0125	.0174		.447	660
	1.0	.001		.230	5.28E+4
1900	.0001	.02	.014	.014	.5
	.001	.0199		.044	5
	.0125	.0174		.136	61
	1.0	.001		.07	4877

dimensionless injection parameter, I, varied with time and distance at various instances in this study. Additionally, it shows the satisfaction of the stability criteria (K less than 0.619) and how the difference between the heat reduction for flat plate and plane stagnation flow near the stagnation point was small (J less than 0.1). Finally, a range of calculated Reynolds numbers based on boundary layer edge conditions are listed to indicate the laminar nature of the leading edge boundary layer.

The film cooling relations required similar treatment. An assumed transient coolant distribution for $\dot{w}_{COOL}$ in Equation (28) was required. Unlike the transpiration cooling model, which assumed coolant injection along the entire leading edge length, the film cooling model was developed based upon coolant injection only along the leading edge stagnation line. Thus, no surface distance relationship for $\dot{w}_{COOL}$ was appropriate for this study. The assumed transient distribution for $\dot{w}_{COOL}$ is shown in Figure 4.6. This data was also placed into a file for the computer model use.

Thus, by indicating whether transpiration or film cooling was to be used with heat pipe cooling, Equation (5) was modified in the computer model. In turn, this selection adjusted the calculations associated with Equation (4), the leading edge surface temperature calculations, and the remaining finite difference numerical results. In Equation (6), ϵ=0.85 was used for all calculations and it was further assumed that the presence of the coolant on the surface did not significantly change its value.

Within the heat pipe structure itself the computational technique known as the alternating-direction-implicit method was used to write the two-dimensional, transient

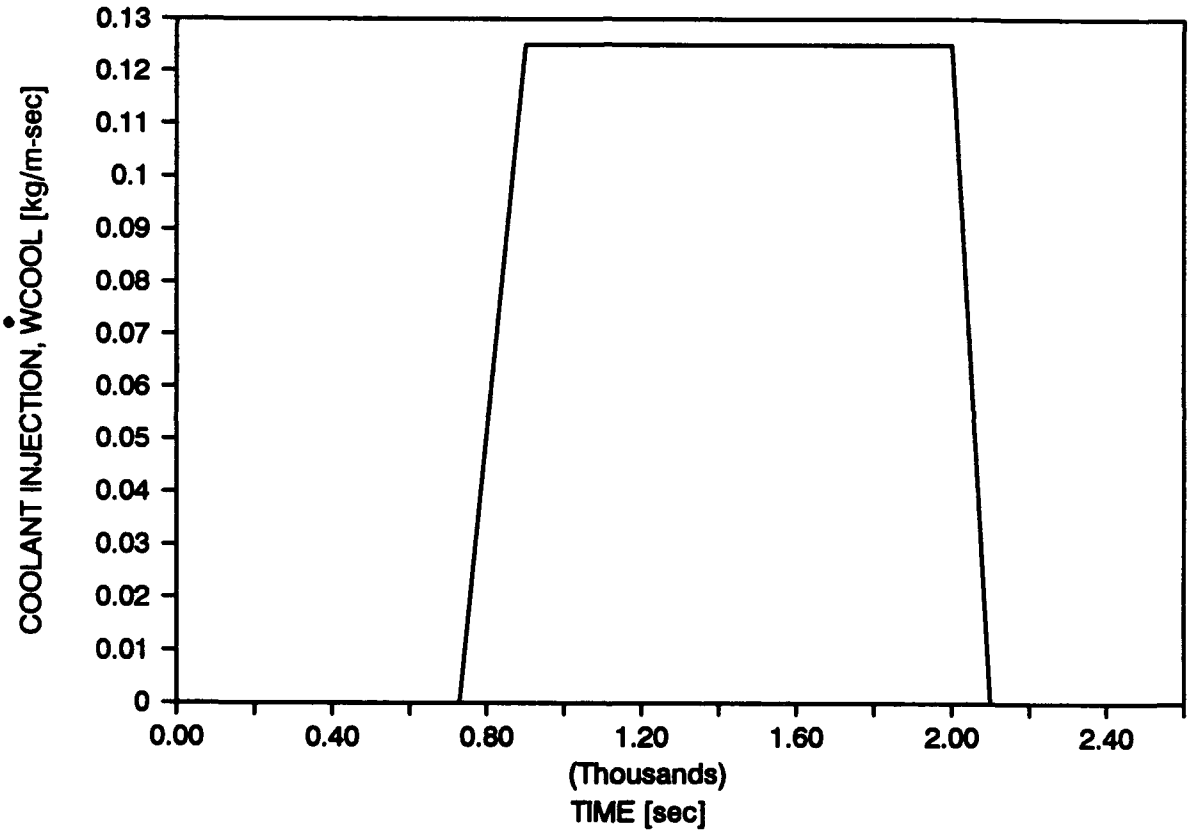

FIGURE 4.6. Transient Film Coolant Injection Profile

finite difference equations. Two systems of non-homogeneous, linear, algebraic equations were obtained by alternately holding temperatures in one spacial direction constant during the first half of a time step and allowing temperatures in the other direction to vary. Then, during the second half of the time step apply the same procedure, but reverse the direction.

Solutions to the finite difference equations were obtained by moving forward in time from a given temperature distribution. The solutions to the first set of equations, from the first half of the time step, were used to solve the second set of equations, yielding the temperature distribution after a full time step. The advantage of the solution method is that it is unconditionally stable as long as the size of the half time step remains unchanged during any given full time step. Time increments can be increased in order to reduce computation time, but excessively large increments can introduce large errors in the calculated temperature distributions. A time increment of 0.1 second was used in the present study.

The leading edge was subdivided into finite difference nodes as shown in Figure 4.7. A total of 40 chordwise direction (x-direction) nodes were used in which 20 were concentrated near the stagnation region to give better definition in this critical area. Five normal direction (y-direction) nodes were used for the shell and two for the capillary structure.

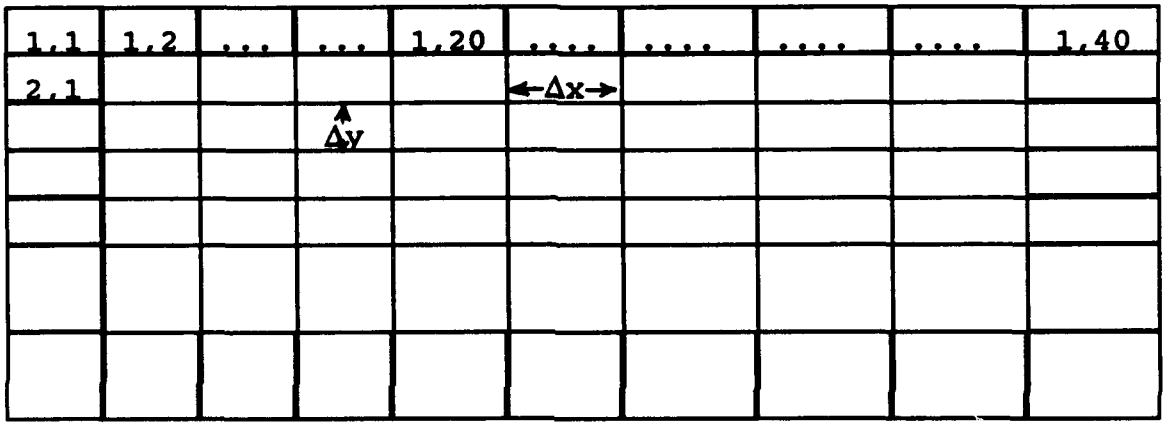

FIGURE 4.7. Schematic of the Leading Edge Finite Difference Nodes

Hypersonic Wing Leading Edge Cooling

An application of the hypersonic leading edge cooling model was then conducted. Helium, water vapor, and air were selected as coolants for this investigation. The selection of these particular coolants was based on a potential availability consideration and on a range of specific heat versus molecular weight basis rather than any predetermined idea of possible candidate coolants for future applications. A coolant reservoir temperature was arbitrarily selected at 600 K for determination of specific heats. No liquid transpiration or film cooling was considered in the present study.

The results of incorporating the hypersonic leading edge cooling model to the wing conditions outlined above are shown in Figures 4.8 through 4.13. Figures 4.8 through 4.10 show predicted transient leading edge surface stagnation temperatures, chordwise-direction surface temperature gradients, and normal-direction skin/heat pipe shell structural temperature gradients at the stagnation point for the case of heat pipe/transpiration cooling using the three coolants with no internal active heat exchanger. Figures 4.11 through 4.13 show the corresponding results for the case of heat pipe/film cooling. For comparison, these figures include results showing heat pipe cooling alone (no internal heat exchanger cooling, no surface mass transfer cooling) and results showing heat pipe/heat exchanger cooling only (no surface mass transfer cooling). The assumed internal active heat exchanger transient heat load used in those results is shown in Figure 4.14.

It has generally been reported that the maximum allowable surface temperature of

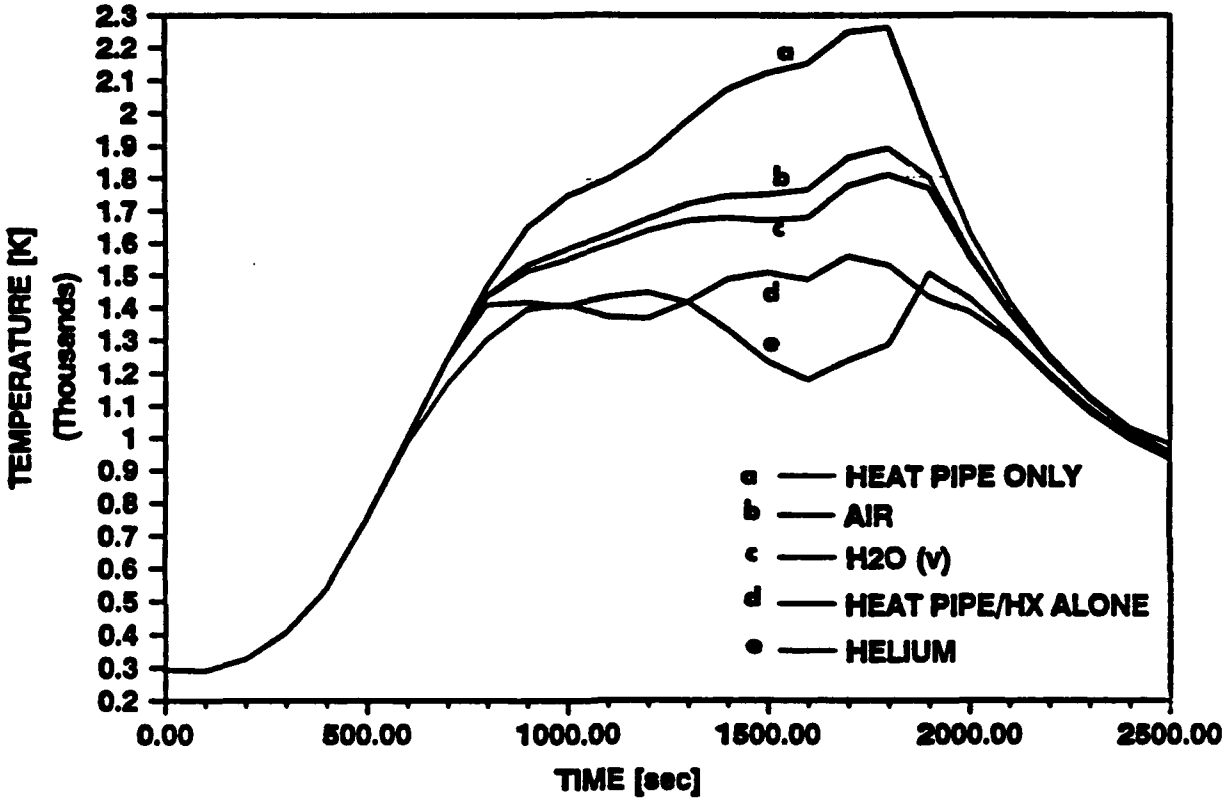

FIGURE 4.8. Transient Surface Stagnation Temperatures Using Transpiration Cooling

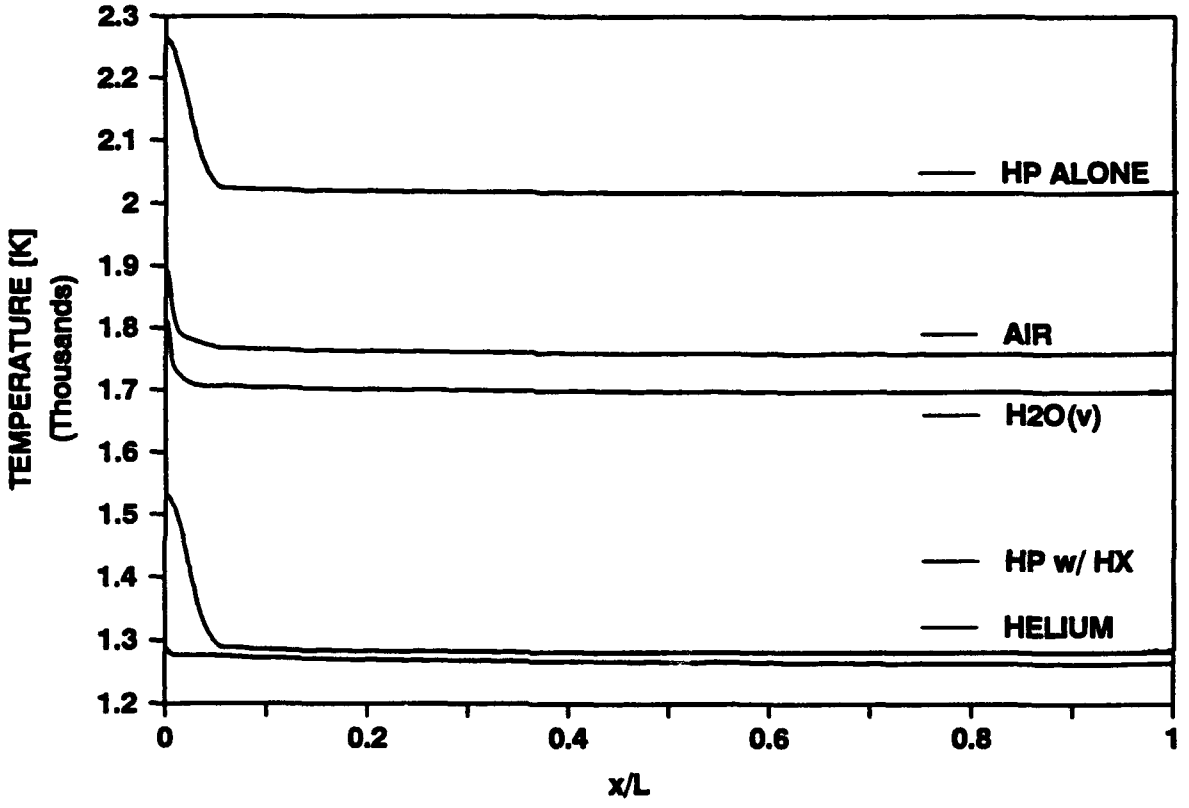

FIGURE 4.9. Chordwise Direction Surface Temperature Gradients Using Transpiration Cooling (Mission Time of 1800 seconds)

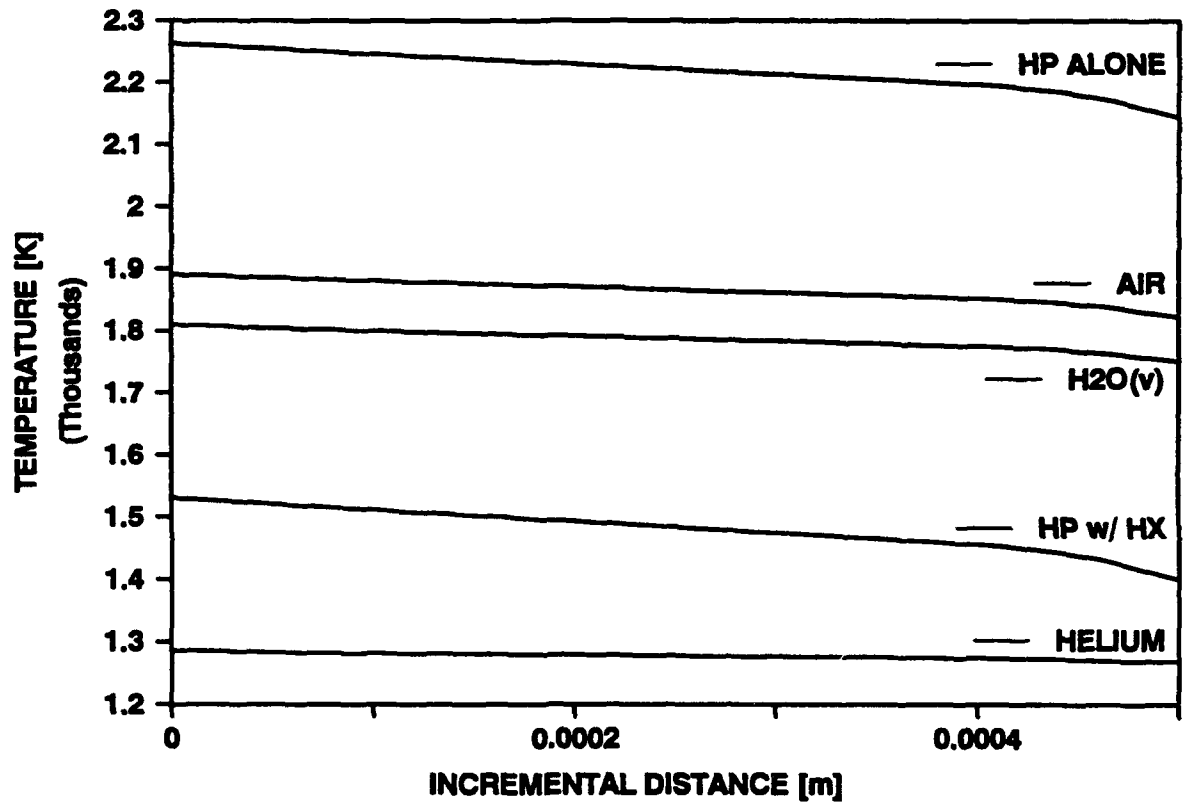

FIGURE 4.10. Normal Direction Stagnation Point Temperature Gradients Using Transpiration Cooling (Mission Time of 1800 seconds)

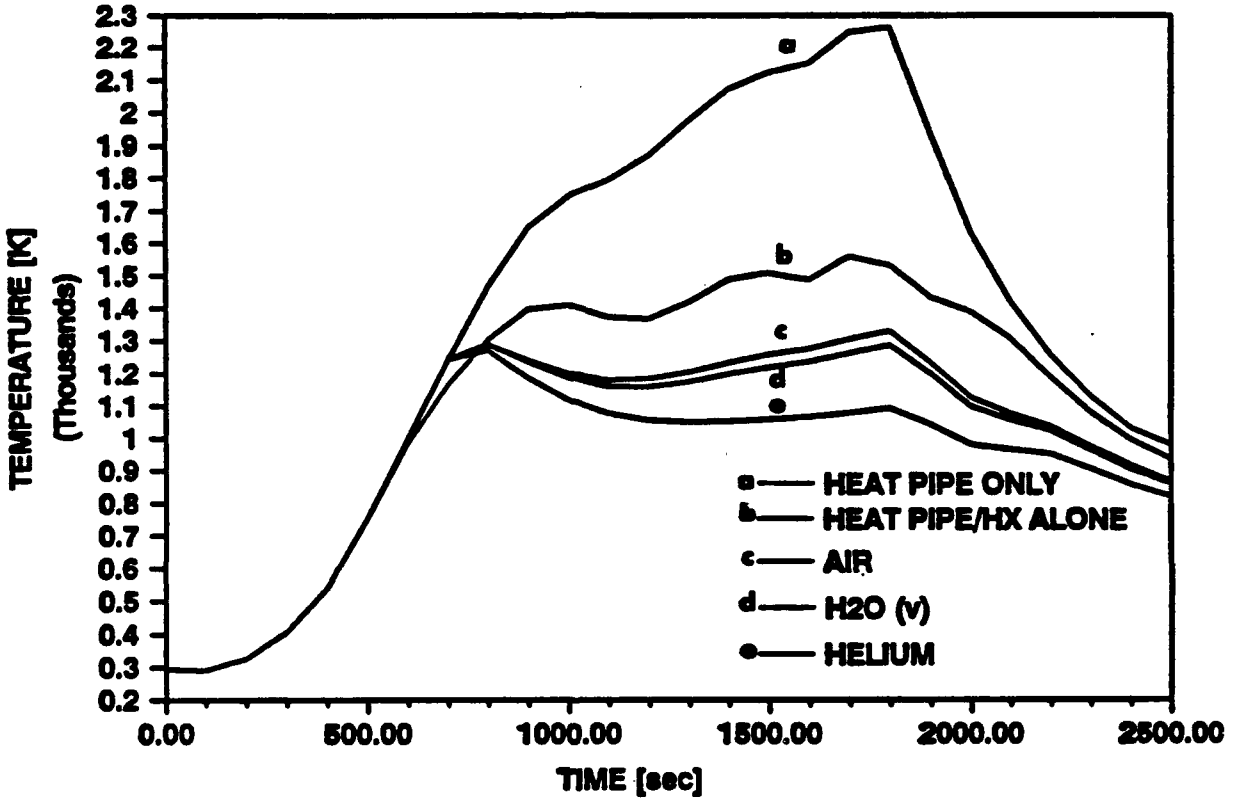

FIGURE 4.11. Transient Surface Stagnation Temperatures Using Film Cooling

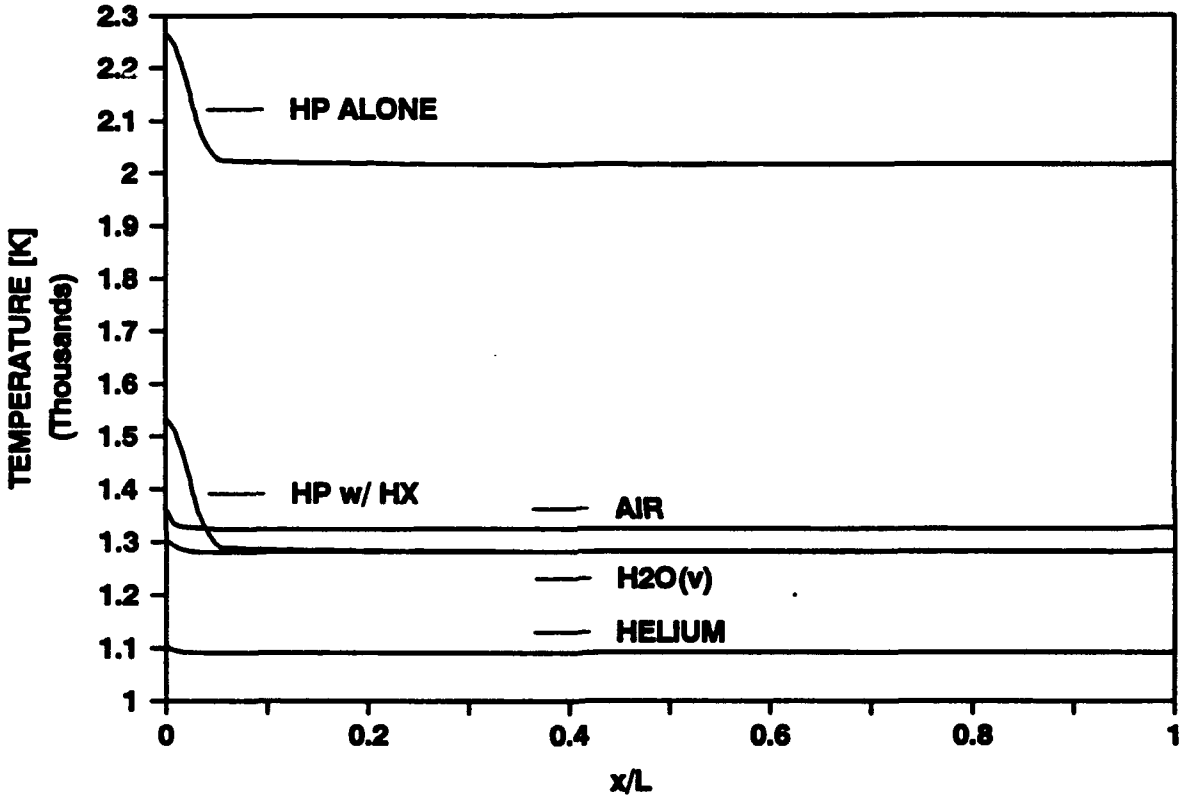

FIGURE 4.12. Chordwise Direction Surface Temperature Gradients Using Film Cooling (Mission Time of 1800 seconds)

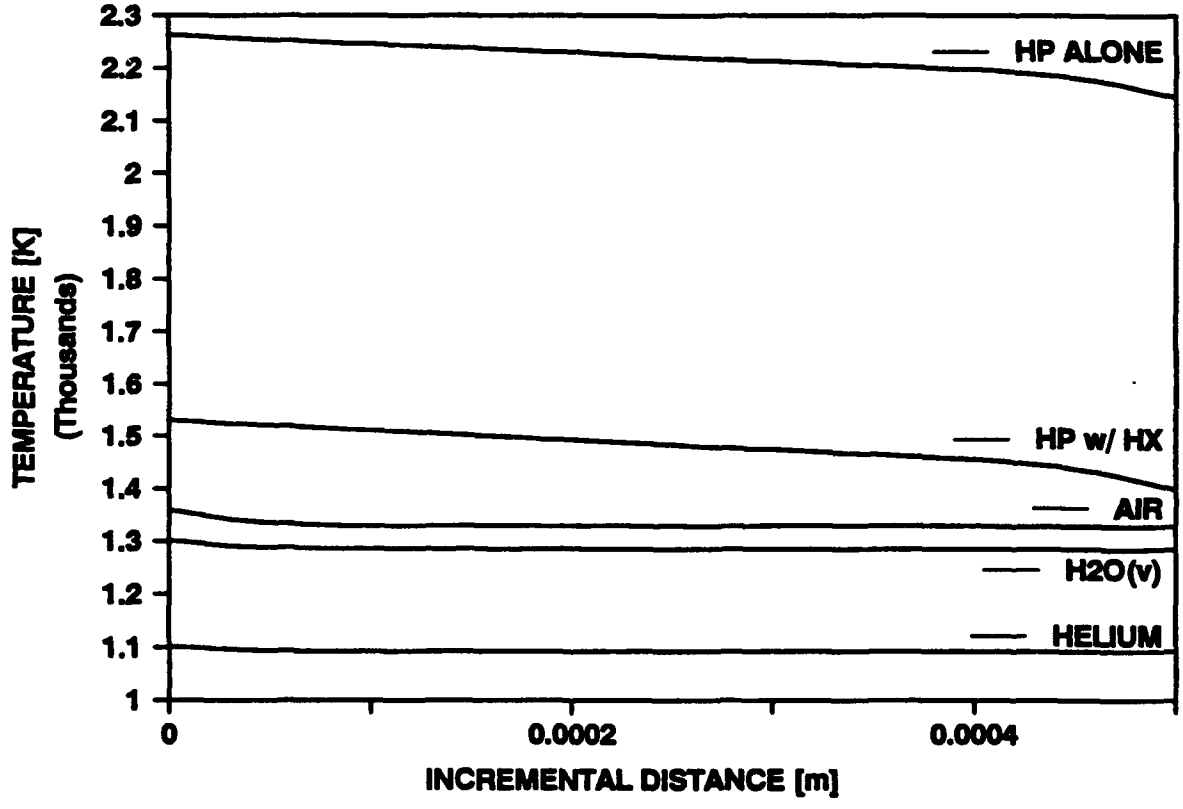

FIGURE 4.13. Normal Direction Stagnation Point Temperature Gradients Using Film Cooling (Mission Time of 1800 seconds)

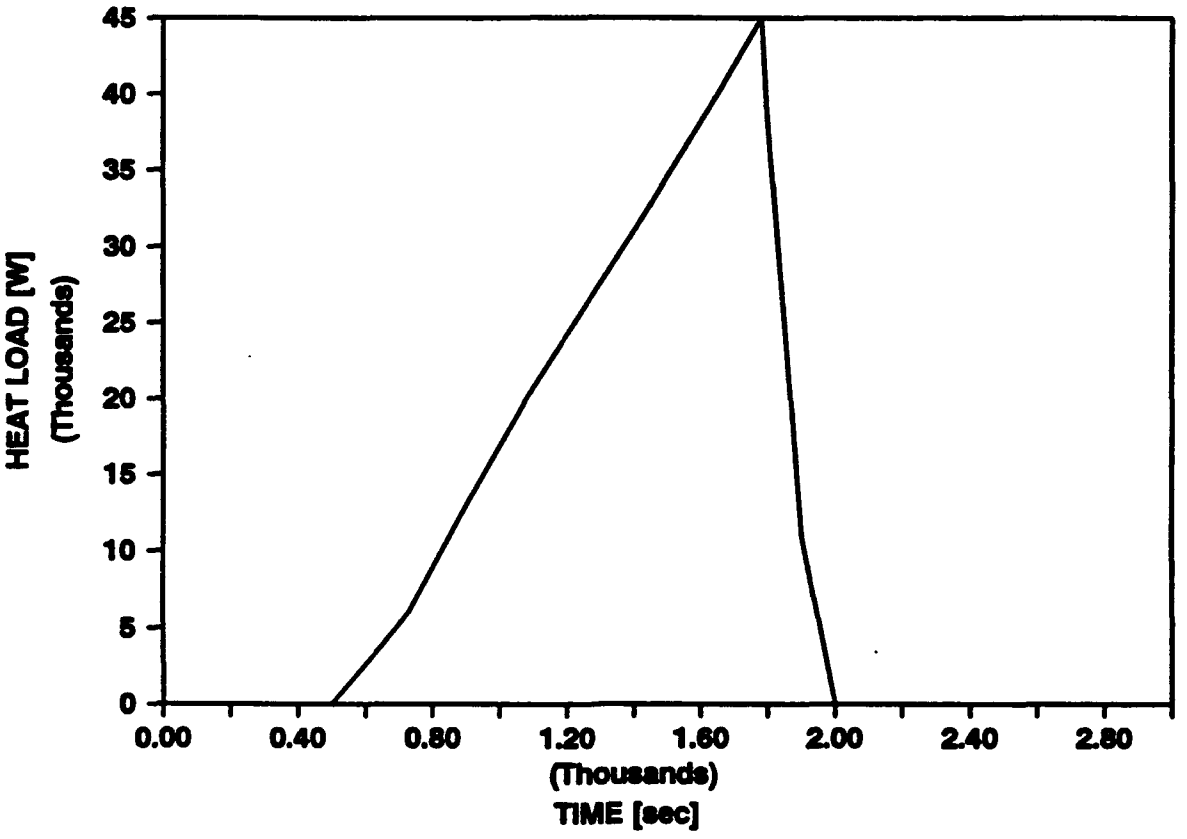

FIGURE 4.14. Assumed Active Internal Heat Exchanger Transient Heat Load

available aero-structural materials is between 1500-1800 K [102]. Given this criteria, Figures 4.8 and 4.11 demonstrate the insufficiency of using liquid metal heat pipes alone to cool the wing leading edge from approximately 700 seconds to 2000 seconds for this typical hypersonic vehicle ascent mission. During this critical window, supplemental leading edge cooling options are required, such as, internal active heat exchanger cooling, surface mass transfer cooling, or a combination of both.

Transpiration Cooling

Figure 4.5 illustrates that for this study the transpiration cooling was initiated and completed to approximately coincide with the critical ascent cooling window from 700 to 2000 seconds. Figures 4.8 through 4.10 indicate that leading edge heat pipe/heavy gas transpiration cooling, under the conditions of this study, are marginally acceptable. Heat pipe cooling supplemented by either an internal active heat exchanger or a transpiring light weight/high specific heat gas appears to be fully adequate. In order for the heavier/lower specific heat gases to be more acceptable, two alternatives are available: either an internal heat exchanger should be used in conjunction with the transpiration cooling, or the amount of transpiration coolant injected into the boundary layer should be increased.

For the first alternative, the required heat exchanger heat load could be reduced from that shown in Figure 4.14. This, in turn, would reduce the heat exchanger coolant mass flowrate requirements and significantly ease the potential heat exchanger/internal leading edge design problems mentioned in the last chapter. In the second case, the use of the

internal heat exchanger is totally unnecessary. However, the amount of increase of transpiration coolant injection requires careful consideration. First, care must be taken to insure that the laminar boundary layer is not destabilized due to the resultant increase of coolant mass from the leading edge surface. If this destabilization occurs, the result could be a significant increase in the heat transfer to the leading edge surface, yielding higher surface temperatures than predicted. Second, the increase of coolant transpiration should not result in a condition which falls outside the limits imposed by Equation (12).

Another important consideration in the design of the leading edge structure will be the effect of thermally induced stresses. One indication of the potential severity of these stresses is the presence of structural temperature gradients. Figures 4.9 and 4.10 show, respectively, the predicted chordwise direction leading edge surface temperature gradients and the normal direction leading edge skin/heat pipe shell stagnation point temperature gradients for the mission time of 1800 seconds. At this time the leading edge stagnation point aerodynamic heat flux was approximately a maximum. Again, the heat pipe alone and heat pipe/heat exchanger only results are indicated for comparison.

Figure 4.9 demonstrates the characteristic near isothermal operation of heat pipe cooling. There appears to be, however, a rather significant surface temperature gradient at the leading edge stagnation region for the heat pipe alone and heat pipe with heat exchanger only cooling methods. As shown in Figure 4.3, this is not surprising because of the severe aerodynamic heating in this region from x/L equal to 0 through approximately 0.05. Figure 4.9 also indicates the severity of this chordwise direction

surface temperature gradient can be mitigated by the introduction of surface transpiration cooling. The coolant effectively blocks some of the heat from being transferred to the surface, thus reducing the surface temperatures. This effect, in conjunction with the heat pipe cooling action, decreases and tends to level out the surface temperature gradients.

Figure 4.10 shows the predicted leading edge skin/heat pipe shell normal direction temperature gradient at the stagnation point. The "0" point in the figure represents the stagnation point surface temperature. In this direction there appears to be less severe structural temperature gradients. Again, the presence of the transpiration cooling only effects the stagnation point surface temperatures. Since the leading edge cooling model of this study assumes that heat is transferred through the structure by conduction only, the individual finite difference nodes in the normal direction would be affected accordingly by this surface temperature reduction.

Film Cooling

Figure 4.6 illustrates that film cooling was also initiated and completed in this study to approximately coincide with the critical leading edge ascent cooling window. Figures 4.11 through 4.13 indicate that all of the heat pipe cooling supplemented with film cooling cases appear to be acceptable alternatives for cooling the wing leading. Again, these figures show, for comparison, the same heat pipe cooling alone and heat pipe with heat exchanger cooling only results as shown in the transpiration cooling case. The results illustrated in Figure 4.11 suggest that for all of the selected coolants no internal heat exchanger cooling may be required with the heat pipe/laminar film surface cooling.

Additionally, Figures 4.12 and 4.13 show similar structural temperature gradient moderations as did the transpiration cooling case.

However, despite this apparent heat transfer reduction the laminar film cooling provides, it has also been reported that excessive upstream coolant injection may destablize the laminar boundary layer, lead to premature transition, and result in subsequent surface heat transfer rates that are significantly greater than those rates corresponding to the no coolant injection case [45,51,73]. Recall, though, for the range of values of $\dot{w}_{COOL}$ used in the experimental work of Redeker and Miller [23], very little coolant film mixing with the free stream flow was reported over a surface distance of 16.6 inches. Referring to Figure 4.6 and Table 4.1 shows that the values of $\dot{w}_{COOL}$ used in the present study also fall within that range, under similar operating conditions, and using a similar leading edge geometry.

CHAPTER V

COOLING MODEL APPLICATION: SCRAMJET ENGINE INLET

It has generally been accepted that the proposed aerospace plane will rely primarily on an air-breathing propulsion system provided by supersonic combustion ramjet engines (SCRAMJETS) for transatmospheric hypersonic flight [103]. An important design aspect of the aerospace plane, which distinguishes it from conventional subsonic or supersonic aircraft, is the integrated airframe-propulsion concept. For conventional aircraft, the components which provide lift (wings), thrust (engines), and volume (fuselage) are separate and distinct. They are easily identifiable on the aircraft and can usually be treated as separate aerodynamic bodies, with moderate interaction, when combined for a total aircraft system design and analysis.

In contrast, the proposed aerospace plane, as shown in Figure 5.1, involves a careful integration of the SCRAMJET engine with the aerodynamic shape of the vehicle itself to allow enhanced propulsion system performance. This integrated airframe-propulsion concept utilizes the entire vehicle underbody as part of the SCRAMJET. Initial compression of the air occurs as a result of passage through the vehicle's nose bow

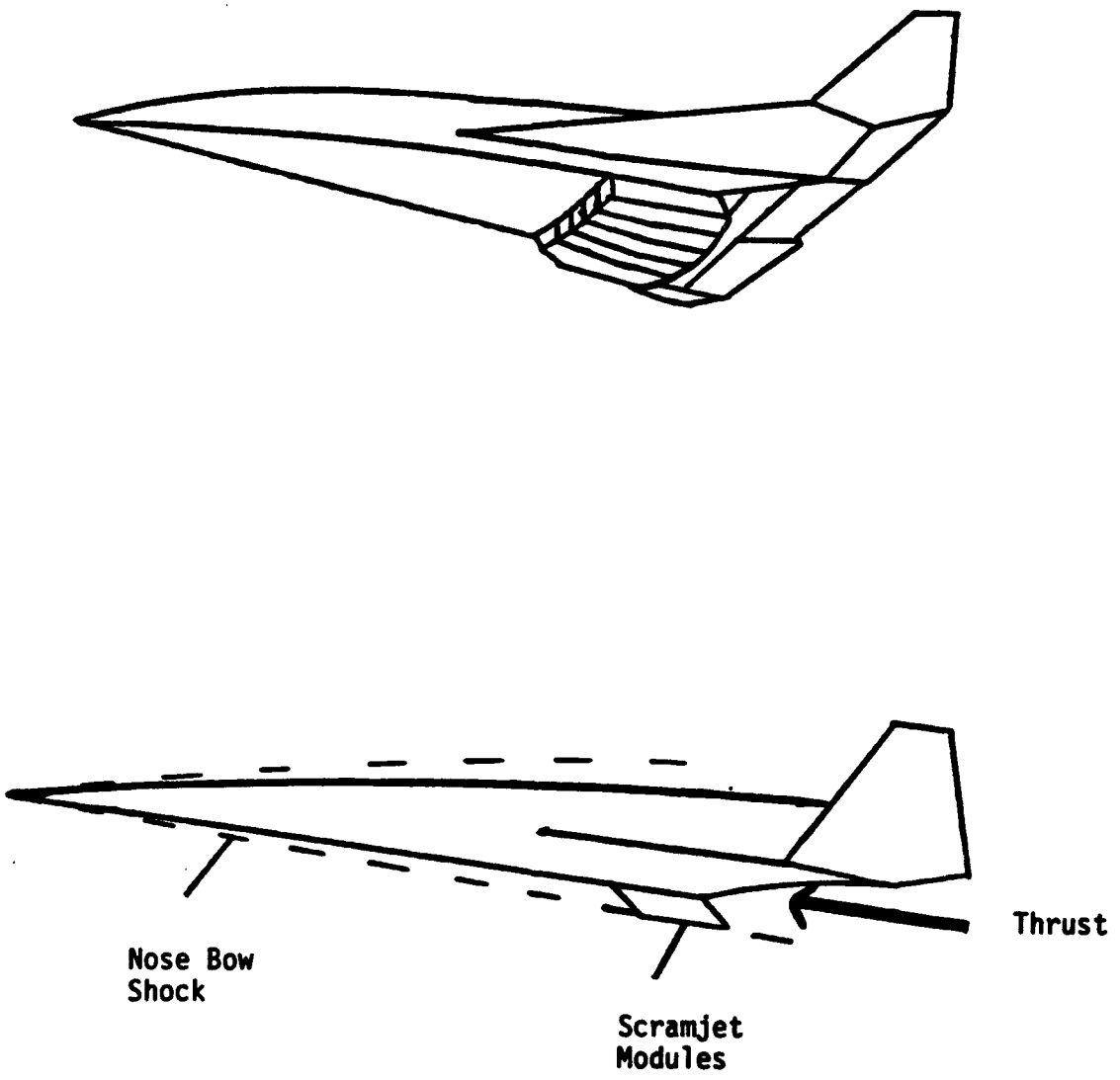

FIGURE 5.1. Hypersonic Aerospace Plane Integrated Airframe-Propulsion Concept

shock. Additional compression and the combustion process take place inside a series of engine modules located near the rear of the vehicle. Primary expansion of the combustion gases occurs over the vehicle's nozzle shaped bottom rear surface. The SCRAMJET engine modules are part of an overall annular inlet area that traverses the vehicle undersurface and is designed to capture enough air to provide the required thrust.

However, an inevitable result of the integrated airframe-propulsion concept is the intersection of the vehicle's nose oblique shock with the engine inlet leading edge (cowl) bow shock. This was not necessarily the case for the wing leading edge, as analyzed in Chapter IV. In an attempt to better understand this interaction phenomena, Edney [104] defined six types of shock interference patterns the intersection creates. Furthermore, it has been demonstrated that these patterns can result in highly localized and intense surface heat transfer rates on the engine cowl leading edge [105-108]. As discussed before, all hypersonic vehicle leading edge surfaces experience intensified stagnation point pressures and heating rates. These loads can be further amplified by an order of magnitude when the leading edge bow shock is impinged upon by an oblique shock wave and results in a Type IV shock interference pattern [106]. Thus, shock interference heating is an additional problem encountered when considering hypersonic vehicle leading edge cooling. This is especially the case for SCRAMJET engine inlets because of their location on the aircraft and the already increased aerodynamic surface heating due to their required, very sharp leading edge geometries.

Motivated by the results discussed in Chapter IV on applying the hypersonic vehicle

leading edge cooling model to a typical wing leading edge, a further investigation was conducted to study the feasibility of applying these same cooling techniques to an aerodynamically heated SCRAMJET engine inlet leading edge also exposed to transient Type IV shock interference heating.

Engine Inlet Model Development and Analysis

It has been demonstrated that the supersonic jet surface interaction (the Type IV shock interference pattern) yields the most severe heat transfer rates and, consequently, has been the focus of the majority of recent research in this area [108]. Dechaumphai, et al., [107] report on a study of the thermal-structural response of a 0.25 inch diameter, internally cooled leading edge subjected to intense shock wave interference heating. The scenario analyzed in their report represented the acceleration of a hypersonic vehicle through Mach 16 with the engine inlet leading edge being exposed to a Mach 8 flow behind the Mach 16 shock front. As the vehicle accelerated through Mach 16, the nose oblique shock was assumed to sweep across the engine inlet leading edge region at a speed of approximately two inches per second. The nose oblique shock intersected the engine leading edge bow shock and produced transient Type IV shock interference surface heating. The envelope for the peak heating values and surface distributions used in their study were idealizations of the experimental data given by Holden, et al., [106]. After the oblique shock swept by, the engine leading edge was then assumed to be heated by the Mach 16 free-stream flow.

For the present investigation, the shock interference scenario and data used in the Dechaumphai, et al., [107] study were also applied. The leading edge illustrated in Figure 3.1 now represented a typical SCRAMJET engine inlet leading edge. It was assumed that this leading edge had generally the same geometric shape, liquid metal heat pipe structure, and was exposed to the same hypersonic vehicle flight trajectory as the did the wing in Chapter IV, except, the engine inlet leading edge nose diameter was reduced to 0.25 inches and there was no internal active heat exchanger cooling. Also, it was assumed that Type IV shock interference heating occurred on the engine leading edge surface as the vehicle accelerated through Mach 16 exposing the surface to a Mach 8 flow as indicated in Figure 5.2. For the assumed vehicle ascent flight trajectory shown in Figures 4.1 and 4.2, this condition arose at approximately 900 seconds into the mission.

To apply the hypersonic leading edge cooling model to this SCRAMJET engine inlet cooling scenario, the same type of analysis used for the wing leading edge cooling discussed in Chapter IV was required. Modifications, though, had to be made to further incorporate the transient Type IV shock interference heating assumed to begin at 900 seconds and the sharper leading edge nose radius.

Based on this assumed scenario, from 0 to 900 seconds the engine inlet leading edge was exposed to a free-stream flow that was actually the air flow downstream of the aircraft's nose oblique shock. In Figure 5.2 this is represented as region 2. Region 3 in this figure represents the air flow in the vicinity of the engine inlet leading edge,

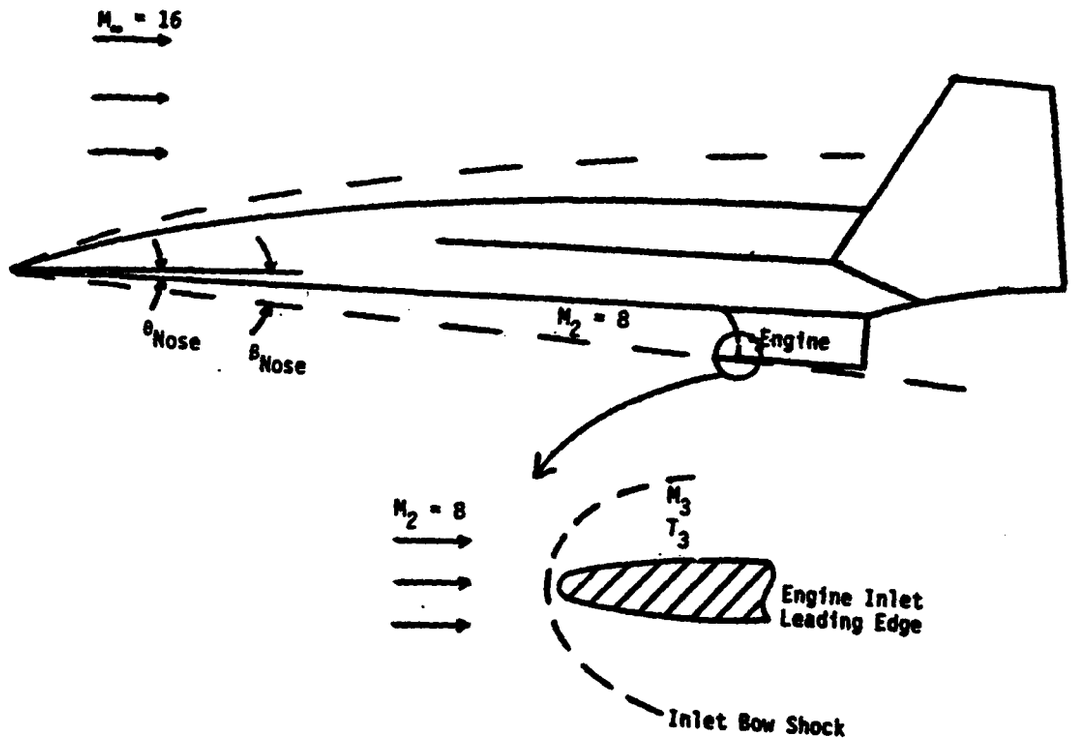

FIGURE 5.2. Assumed Hypersonic Aerospace Plane Configuration at the Mission Time of 900 seconds

behind its leading edge bow shock. As seen in the last chapter, the thermodynamic and flow properties of the air in region 3 are required for use in this application of the leading edge cooling model and their determination is based upon the appropriate upstream properties. Therefore, before region 3 could be analyzed, more detailed information about region 2 had to be determined. Since the region 2 air flow at this time was not greater than Ma=8, standard compressible flow and oblique shock relations were used to calculate the required region 2 air data [96,109]:

$$\frac{T_2}{T_\infty} = \left(\frac{a_2}{a_\infty}\right)^2 = \left(\frac{Ma_\infty}{Ma_2}\right)^2 \left(\frac{u_2}{u_\infty}\right)^2 \tag{33}$$

$$\frac{u_2}{u_\infty} = \frac{(\gamma - 1)\, Ma_\infty^2 \sin^2\beta + 2}{(\gamma + 1)\, Ma_\infty^2 \sin^2\beta} \tag{34}$$

$$\frac{T_2}{T_\infty} = 1 + \frac{2(\gamma - 1)\, Ma_\infty^2 \sin^2\beta - 1}{(\gamma + 1)^2\, Ma_\infty^2 \sin^2\beta} \tag{35}$$

and,

$$\theta \cong \frac{2\beta}{(\gamma+1)}. \tag{36}$$

Substituting Equation (34) into Equation (33) and equating this result to Equation (35) allowed for the solution of β_{NOSE} in Figure 5.2 at $Ma_\infty = 16$. It was determined that $Ma_\infty \beta \gg 1$ for this condition, thus the hypersonic approximation for θ_{NOSE} was made using Equation (36). Having this value for the vehicle's θ_{NOSE} allowed for the determination of the transient region 2 flow-field properties by using standard oblique shock calculations and relationships throughout the mission time interval of 0 to 900 seconds. At 900 seconds, the nose oblique shock was assumed to sweep across the engine inlet leading edge bow shock in approximately 0.2 second and initiate the Type IV shock interference behavior described by Dechaumphai, et al., [107]. After approximately 900.2 seconds the leading edge was exposed to the vehicle's transient free-stream flight conditions shown in Figures 4.1 and 4.2 for the remainder of the mission. That is, from 900.2 to 3000 seconds the region 2 flow-field conditions were, in fact, the ∞-conditions. Flow-field conditions from 900 to 900.2 seconds were assumed to remain constant at the 900 second values.

Therefore, determination of the region 2 flow-field for the entire ascent mission provided the necessary free-stream data to determine the region 3 thermodynamic and flow properties using the same assumptions and techniques discussed in Chapter IV. Once determined, these properties were used, where appropriate, in both the leading edge

cooling model and in the determination of the engine inlet leading edge aerodynamic surface heat flux data.

Figure 5.3 shows the resulting SCRAMJET engine inlet leading edge chordwise direction surface heat flux distribution. Figure 5.4 shows the transient stagnation aerodynamic heat flux used for the inlet leading edge. The data represented on these two figures were also determined using the same assumptions and techniques employed in Chapter IV for the wing leading edge case.

Figure 5.3 incorporates the sharper nose radius assumed for the engine inlet leading edge. This figure also indicates that for the present analysis it was assumed that the maximum surface heating occurred at the leading edge stagnation point. This assumption was reasonable throughout the mission except during the Type IV shock interference heating condition occurring from 900 to 900.2 seconds. Holden, et al., [106] acknowledge that attempting to define the surface location of the peak heating load for a Type IV interaction is difficult. The general trend, though, is that the peak loading occurs on the surface when the supersonic jet surface impingement, from the shock interaction, is approximately 20 degrees below the stagnation point, regardless of Mach number [106]. For the purpose of the present investigation, however, it was felt that due to the short time duration of the assumed shock interference effect, the assumption of the peak heating occurring at the stagnation point would not significantly affect the overall results. Additionally, Figure 5.4 incorporates the smaller engine inlet nose radius and the Type IV shock interference data of Dechaumphai, et al., [107] from 900 to 900.2

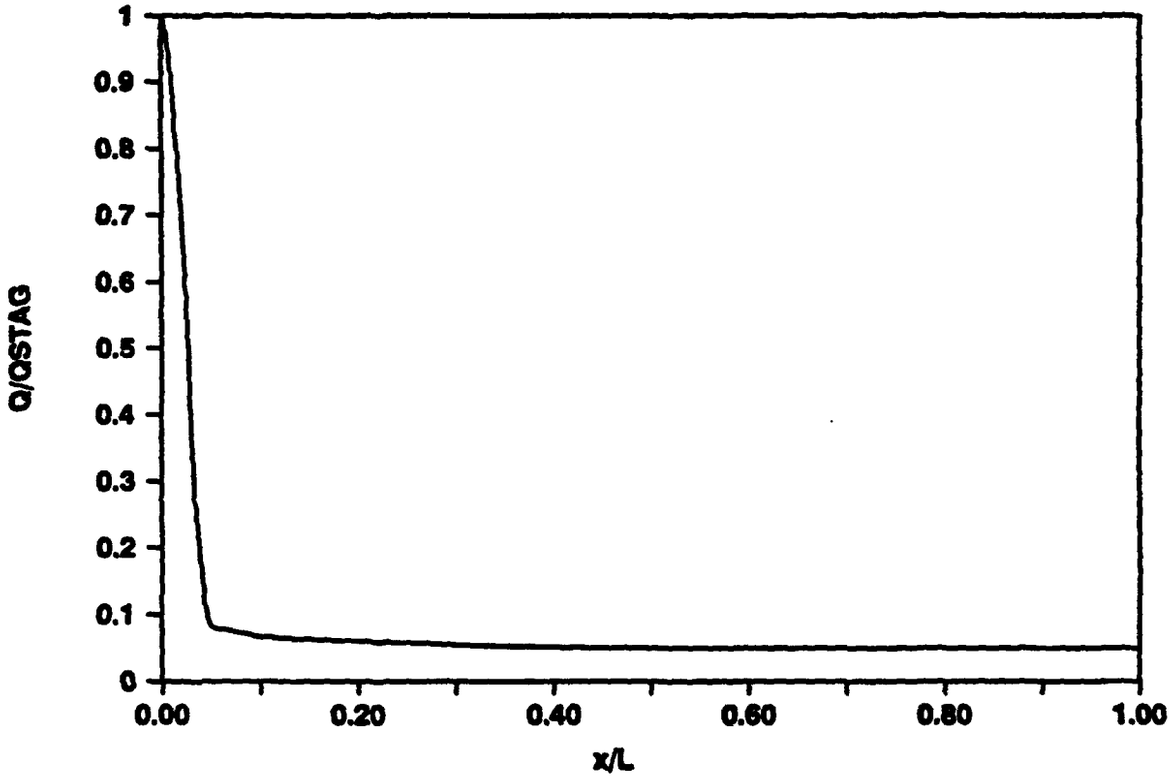

FIGURE 5.3. SCRAMJET Leading Edge Surface Heat Flux Distribution, Chordwise Direction

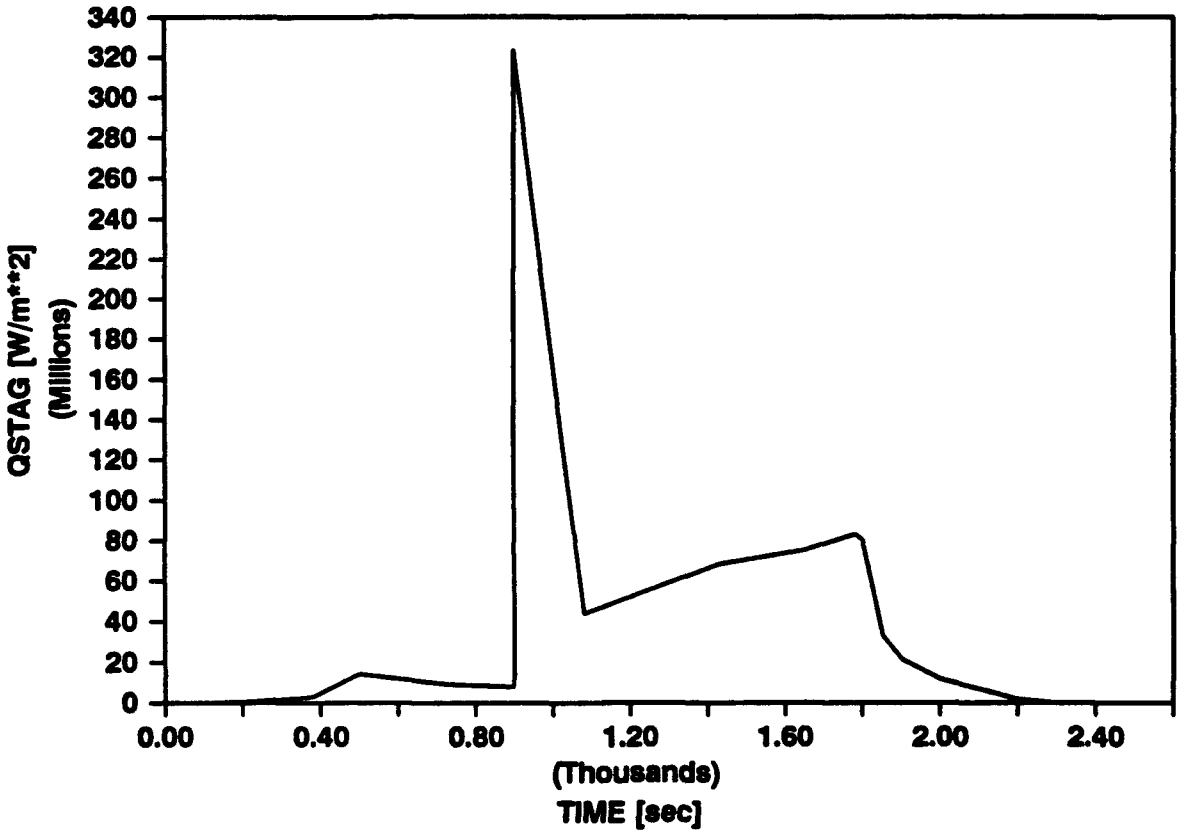

FIGURE 5.4. SCRAMJET Leading Edge Transient Stagnation Aerodynamic Heat Flux

seconds.

Figures 5.5 and 5.6 present, respectively, the transpiration and film coolant injection profiles used for the engine inlet leading edge cooling. Since no internal active heat exchanger was utilized for this application, the coolant injection profile selections were based upon maximizing the coolant flowrate, while still insuring the model limits and boundary layer stability criterium discussed in Chapter IV remained satisfied. Additionally, air alone, at a reservoir temperature of 600 K, was used as the test coolant.

Results

The results of applying the hypersonic leading edge cooling model to the SCRAMJET engine inlet are shown in Figures 5.7 through 5.10. Figures 5.7 and 5.8 show the predicted transient leading edge surface stagnation temperatures for the heat pipe with air transpiration and film cooling cases. For comparison, leading edge cooling using the heat pipe only is also indicated on both figures.

Applying the same 1500 to 1800 K maximum allowable leading edge surface temperature criteria discussed in the last chapter yields a number of observations. First, leading edge heat pipe cooling only is not sufficient during the mission time interval of approximately 450 to 2250 seconds. The temperature spike shortly after 900 seconds on Figures 5.7 and 5.8 corresponds to the Type IV shock interaction effect and represents the maximum leading edge surface temperature during the ascent mission when heat pipe cooling only is used. Second, incorporating air transpiration or film cooling with the

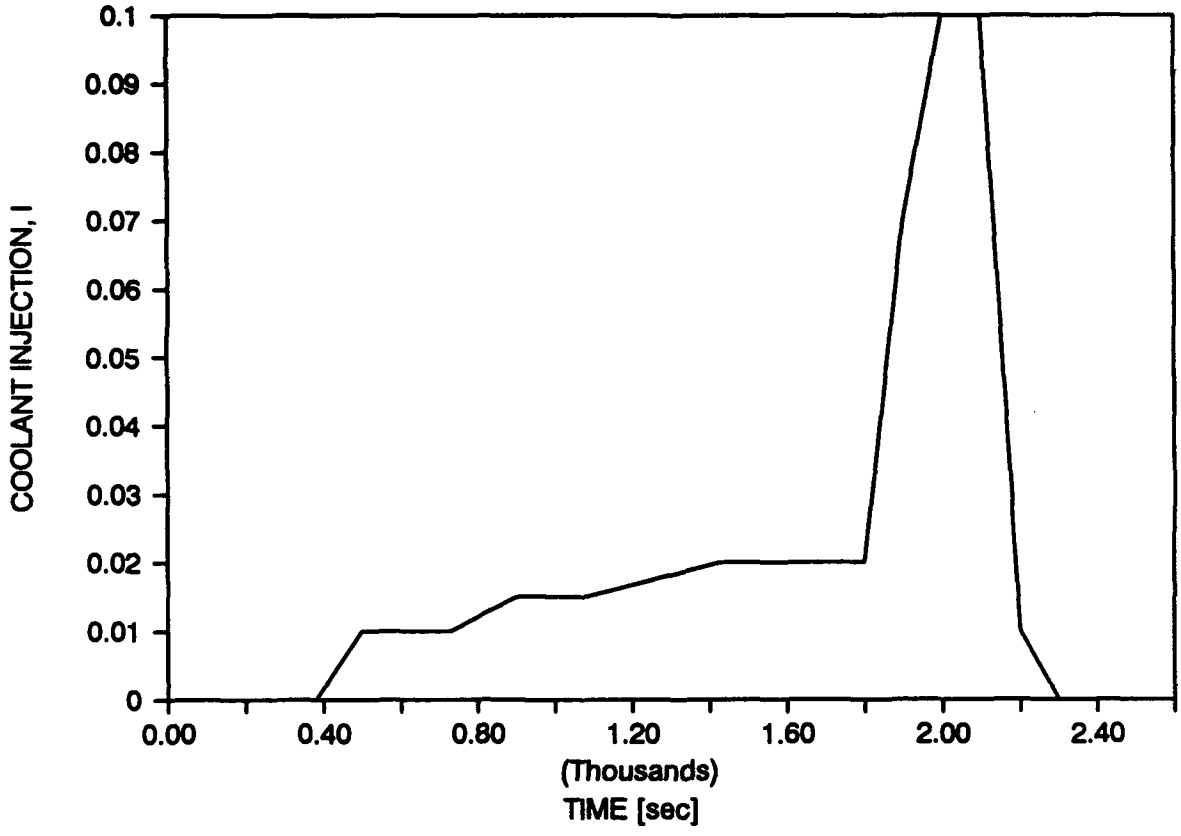

FIGURE 5.5. SCRAMJET Transient Nondimensional Transpiration Coolant Injection Profile

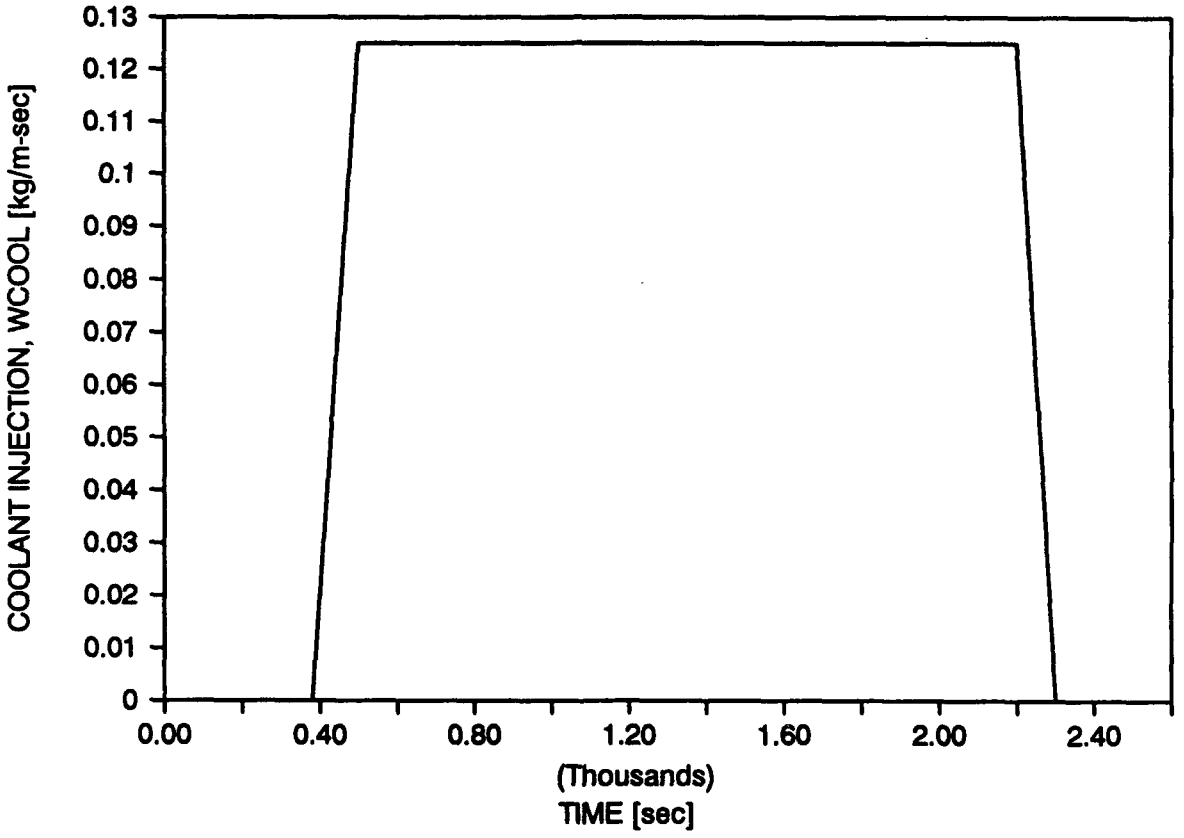

FIGURE 5.6. SCRAMJET Transient Film Coolant Injection Profile

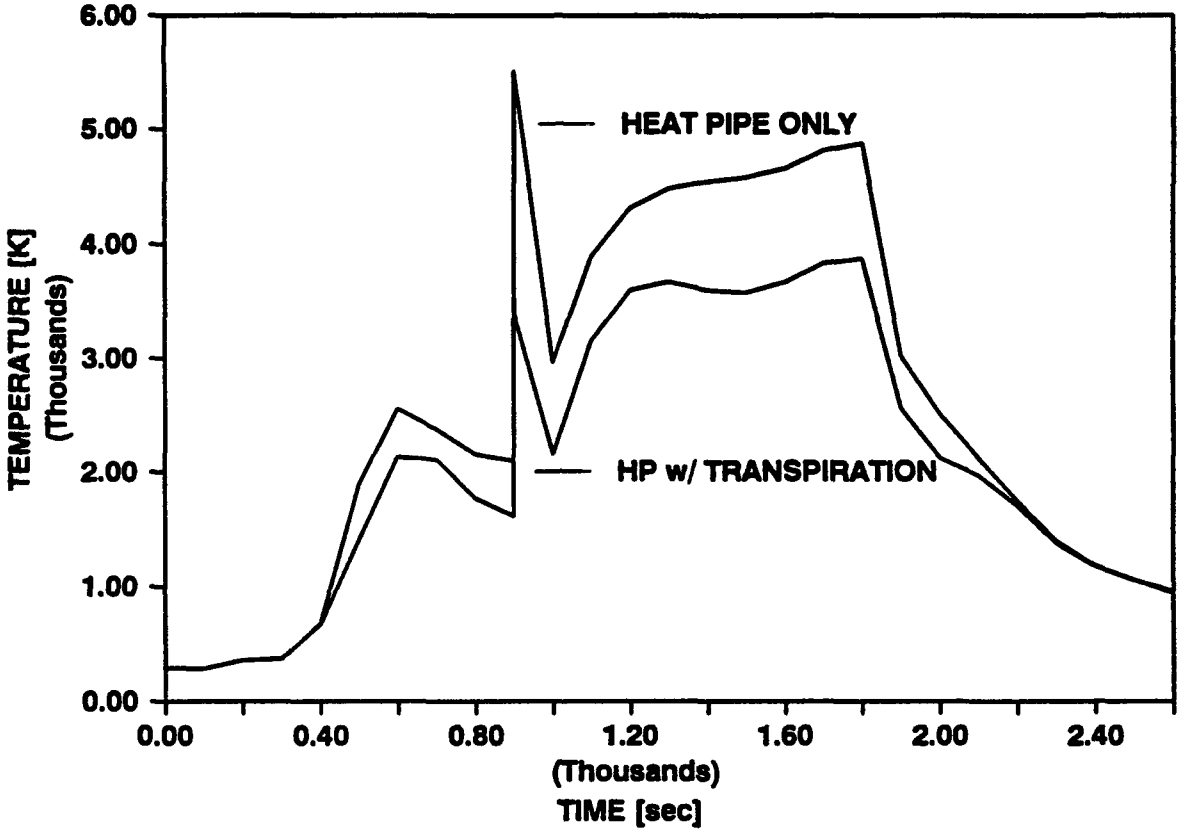

FIGURE 5.7. SCRAMJET Transient Surface Stagnation Temperatures Using Transpiration Cooling

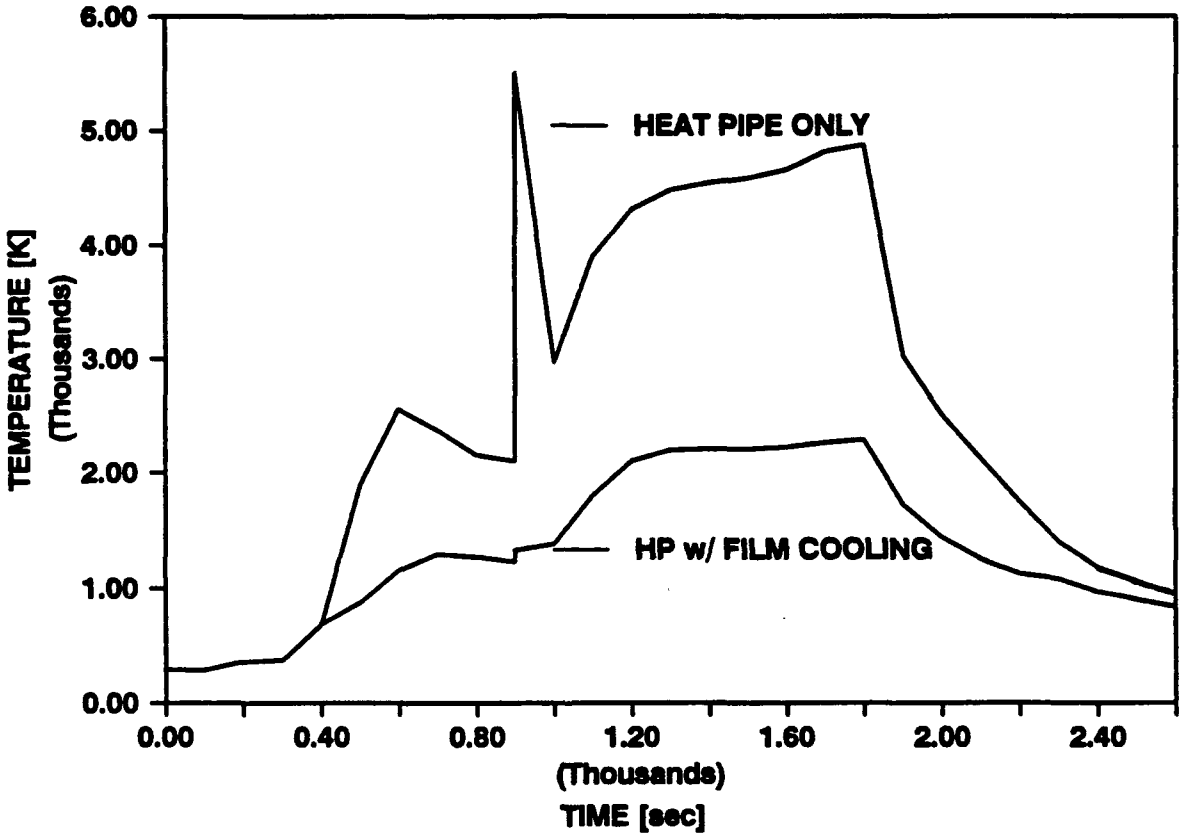

FIGURE 5.8. SCRAMJET Transient Surface Stagnation Temperatures Using Film Cooling

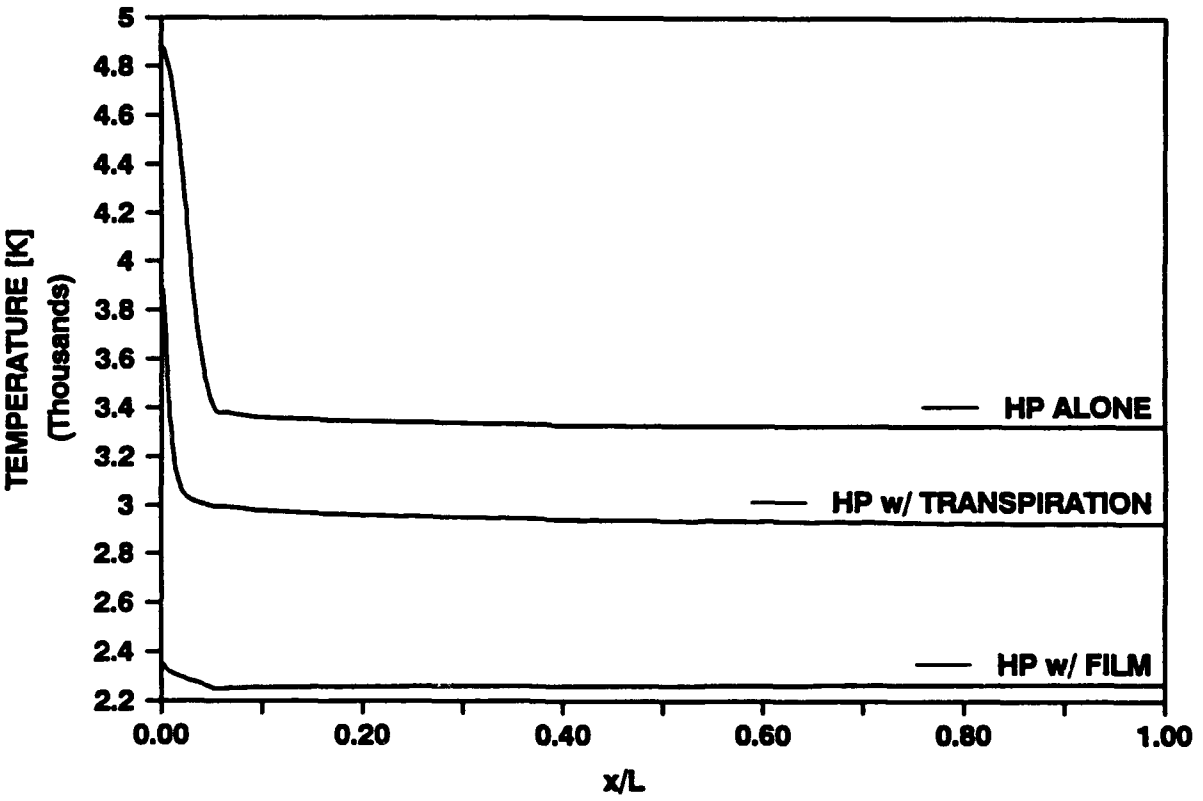

FIGURE 5.9. SCRAMJET Chordwise Direction Surface Temperature Gradients

(Mission Time of 1800 seconds)

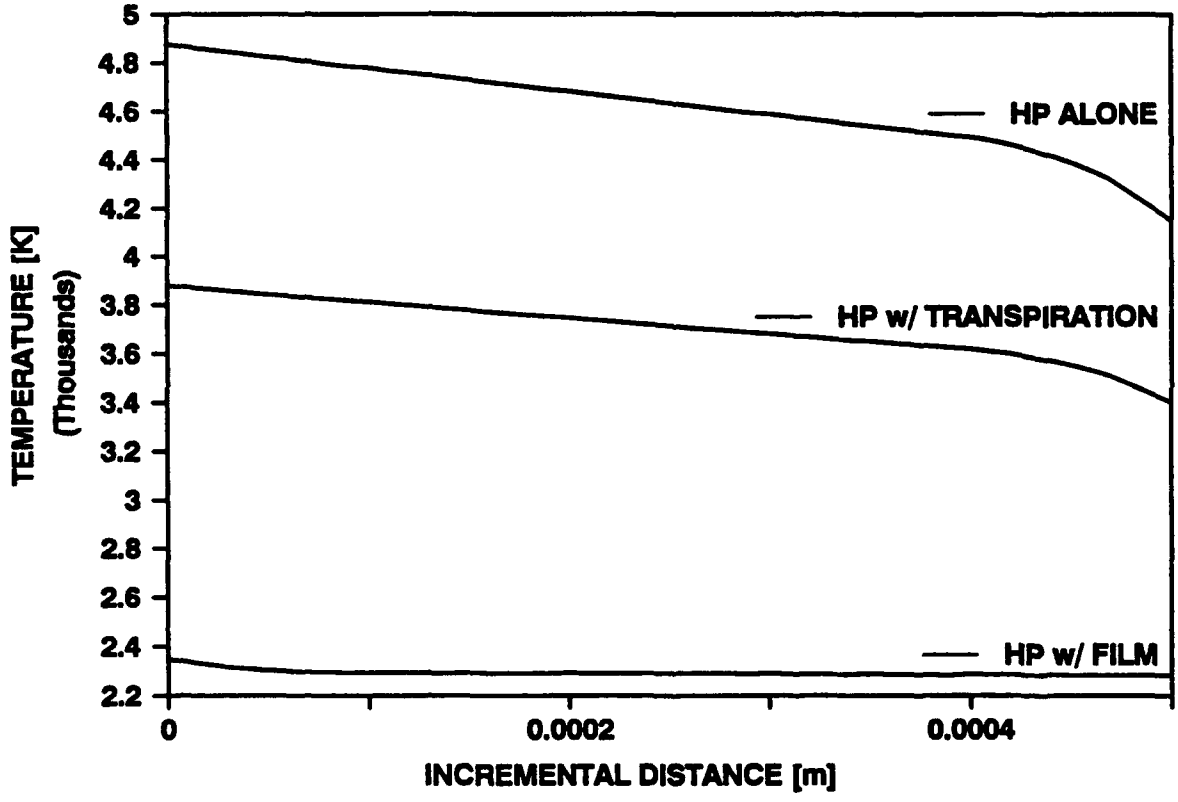

FIGURE 5.10. SCRAMJET Normal Direction Stagnation Point Temperature Gradients

(Mission Time of 1800 seconds)

heat pipe does lower the leading edge surface temperatures, but not into the maximum allowable range. Third, using the heat pipe/mass transfer cooling combination appears to shift the time when the maximum leading edge surface temperature occurs. This shift is away from the shock interaction time and to a time shortly after the mission time corresponding to the occurrence of the maximum aerodynamic surface heat flux for the no shock interaction case. Recall that for the wing leading edge, the maximum surface temperature occurred shortly after the time of the maximum aerodynamic heating. Fourth, the results shown in Figures 5.7 and 5.8 indicate that supplemental transpiration or film cooling tends to reduce the magnitude of the thermal effect from the shock interaction on the surface of the heat pipe cooled leading edge.

Figures 5.9 and 5.10 show, respectively, at the mission time of 1800 seconds the chordwise direction leading edge surface temperature gradients and the normal direction skin/heat pipe shell stagnation point temperature gradients. The time of 1800 seconds was selected since it represented the maximum temperature condition for the transpiration and film cooling cases. Again, as was seen with the wing leading edge, steep surface temperature gradients exist close to the engine inlet stagnation point. Supplemental transpiration and film cooling, however, tended to reduce this condition. The normal direction gradient is similarly affected.

Thus, based upon the assumed conditions in this application, it appears that leading edge liquid metal heat pipe cooling supplemented by surface transpiration or film cooling could be used to mitigate the expected aerodynamic heating effects on a SCRAMJET

engine inlet. Further, it appears that these methods could be used as additional techniques for reducing the potentially severe Type IV shock interaction surface heating effects, along with those discussed by Holden, et al., [106] and Glass, et al., [110]. Applying the trends discussed in the last chapter suggest that the overall engine inlet leading edge cooling effectiveness could be improved by: 1) using some type of an internal active heat exchanger, or 2) using a surface coolant with a lower molecular weight and higher specific heat than that of air. For the second case, the potential effect on engine combustion efficiency would have to be considered due to the trace presence of coolant gas in the combustion air. Hydrogen, perhaps an obvious choice for a surface coolant, is not practical in these applications, however, due to its low combustion temperature (approximately 1100 K) compared to the relatively high maximum allowable leading edge surface temperatures (1500-1800 K) [74].

It must also be re-emphasized that this analysis, as did the wing analysis, assumed the leading edge laminar boundary layer remained attached throughout the entire ascent mission. Although the transpiration and film coolant mass injection rates and distributions used in the study were selected based upon the best available criteria in the literature to ensure boundary layer stability, the potentially severe adverse pressure gradient imposed on this thickened, laminar boundary layer by the shock interaction effect could cause local separation, if not transition to turbulence. Unfortunately, there is a lack of information in the literature regarding this shock/thickened laminar boundary layer due to mass addition interaction.

It is documented, however, that in the absence of mass addition a turbulent boundary layer has a greater capability of withstanding adverse pressure gradients than a laminar one and that this ability increases with Mach number [73]. Ledford and Stollery [73] report the results of a test program intended to evaluate the effect of a shock interaction on a turbulent, film cooled, hypersonic flat plate boundary layer. However, they were only able to conclude what was already known: turbulent film cooling offered little thermal protection to a flat plate. Yet, this conclusion adds confirmation to the desire of maintaining a laminar boundary layer on the leading edge surface.

CHAPTER VI

CONCLUSIONS AND RECOMMENDATIONS

The problem of cooling to an acceptable level hypersonic aerospace plane leading edge structures exposed to severe aerodynamic surface heating was addressed in this investigation. A numerical, finite difference based hypersonic leading edge cooling model incorporating post-startup liquid metal heat pipe cooling with surface transpiration and film cooling was developed to predict the transient structural temperature distributions and maximum surface temperatures of an aerospace plane leading edge. It was envisioned that this model could be used as a tool for future hypersonic leading edge cooling engineering design calculations. Application of this model was demonstrated for two cases: 1) the cooling a typical aerospace plane wing leading edge section, and 2) the cooling of an aerospace plane SCRAMJET engine inlet (cowl) section.

Results of the applications showed that for the wing leading edge, liquid metal heat pipe cooling alone was insufficient for maintaining surface temperatures below an assumed maximum level of 1800 K for approximately one-half of a typical aerospace plane ascent trajectory through the Earth's atmosphere. However, supplementing the

heat pipe cooling with an active internal heat exchanger cooling mechanism, with gaseous transpiration cooling along the entire leading edge length, or with gaseous film coolant injection at the leading edge stagnation point yielded significant improvements. The results also indicated that the injected coolant gas possessing the combination of a high specific heat and low molecular weight provided the greatest aerodynamic heat transfer reduction to the leading edge surface in both the transpiration and film cooling cases. Additionally, surface transpiration and film cooling tended to reduce the magnitude of both the leading edge chordwise direction surface temperature gradients and the normal direction skin temperature gradients at the stagnation point. For the SCRAMJET engine inlet cooling, it was further demonstrated that both transpiration and film cooling tended to mitigate the severe Type IV shock interaction surface heating effect. This was apparently due to the combination of the typically very short time duration and surface locality of this type of shock interaction along with the inherent heat transfer blocking action characteristic of surface transpiration and film cooling.

Although the finite difference based leading edge heat pipe model, the transpiration cooling model, and the film cooling model have been individually correlated and checked with experimental data, there exists no data in the literature, at this time, available to validate the results predicted by this study's combined hypersonic leading edge cooling model. Consequently, confidence in its results has to be based upon the reasonableness of the model's assumptions and the correctness of its applications.

One critical assumption that cannot be truly verified, without the benefit of

experimental data, is the attached laminar leading edge boundary layer assumption. Aerodynamic surface heating calculations, the transpiration and film cooling heat transfer reduction effects, and the criteria for ensuring laminar boundary layer stability in the presence of surface mass addition were all based upon this assumption. Yet, there does appear to be some validation for the assumption besides the data and discussion presented in the body of this report. It has been experimentally shown on a 5 degree half-angle cone, with a trajectory having a dynamic pressure of 1000 psf, that high Mach number flows tend to laminarize the surface boundary layer [111]. Recall, for the present investigation of high Mach number flows over a sharp-nosed leading edge the dynamic pressure was assumed to be 2000 psf. Therefore, it would be reasonable to assume that the increased dynamic pressure used in this study would yield an increased tendency to laminarize the leading edge surface boundary layer and, thus, provide further confidence in assuming laminar boundary layer flow.

Also related to the boundary layer issue is the possible effect on laminar heating by the so-called "high-entropy gas layer" typically associated with hypersonic flow over blunt bodies. In the present investigation this effect was not considered significant. Unlike what is experienced on the blunter space shuttle leading edges, it is felt that the much sharper nose of the aerospace plane would largely eliminate the high-entropy layer and that flat plate approximations would yield more reasonable laminar heating values [94].

Lastly, no attempt has been made in this study to compare to one another the relative

cooling effectiveness of the transpiration and film cooling cases. This would require, among other things, knowledge of the specific coolant mass flowrates necessary to give the heat transfer reduction results presented in Chapters IV and V. Since the surface injection geometry required for these two methods is completely different, as shown in Chapter II, the coolant injection requirements in the present investigation were developed on a mass flux basis. Therefore, no particular coolant injection geometry for the aerospace plane leading edge surface had to be assumed. Rather, emphasis could be placed on determining the feasibility of each cooling concept without concern over what would be the optimum coolant injection design.

The findings of this investigation have also pointed to areas recommended for future study:

1. A leading edge structure needs to be built and an experimental study conducted which incorporates surface transpiration and film cooling with liquid metal heat pipe cooling of the leading edge when exposed to the flow and surface heating conditions used in the present investigation. This task would help in determining the validity of the hypersonic flow-field, laminar boundary layer flow, and structural cooling assumptions/predictions discussed in the present report. With experimental data such as this, modifications, as necessary, to the leading edge cooling model of the present study could be made.

2. Analytical expressions to account for melting of the heat pipe working fluid should

be incorporated into the leading edge cooling model. This modification would allow the finite difference based model to be used to additionally predict cooling performance during heat pipe startup, similar to the finite element based heat pipe model discussed in Chapter III.

3. The leading edge cooling model needs to be made three-dimensional with respect to heat transfer. To fully study this cooling concept for an entire leading edge span, this modification will eventually have to be done.

4. Studies should be conducted with this model to determine the feasibility of using surface transpiration and film cooling without heat pipe cooling. These studies could be done with or without the supplemental use of an active internal heat exchanger. The results could be interpreted as representing the structural cooling effects of these techniques themselves or used to model the scenario of cooling a leading edge when the heat pipe has failed.

5. A study of the effect various distributions of coolant injection over the leading edge surface on cooling performance should be conducted. Coolant transpiration, for example, could take place only at the stagnation region rather than along the entire leading edge length. This action could possibly decrease the chordwise direction surface temperature gradients predicted in the present study.

6. The effect of increasing or decreasing the leading edge/heat pipe length on this model's cooling performance should be studied. This may be of particular interest in the SCRAMJET engine inlet cooling case.

7. Studies should be conducted to evaluate the response of a thickened laminar boundary layer due to surface mass addition to Type IV shock interactions.

8. The use of liquid surface coolants should be investigated. The added energy absorption provided by the liquid's heat of vaporization would improve this concept's potential cooling effectiveness. However, particular attention to the complications associated with maintaining a thin, liquid film on a surface exposed to a hypersonic environment needs to be considered [28,64,112,113].

REFERENCES

1. Tien, C.L., "Fluid Mechanics of Heat Pipes", Annual Review of Fluid Mechanics, ed. M. Van Dyke, W.G. Vincenti and J.V. Wehausen, Vol. 7, Annual Reviews, Palo Alto, CA, 1975, pp. 167-185.

2. Grover, G.M., "Evaporation-Condensation Heat Transfer Device", U.S. Patent 3229759, Dec 1963.

3. Deverall, J.E. and Kemme, J.K., "High Thermal Conductance Devices Utilizing the Boiling of Lithium or Silver", LA-3211, Apr 1965.

4. Cotter, T.P., "Theory of Heat Pipes", LA-3246-MS, Feb 1965.

5. Sun, K.H. and Tien, C.L., "Thermal Performance Characteristics of Heat Pipes", International Journal of Heat and Mass Transfer, Vol. 18, 1975, pp. 363-380.

6. Chang, W.S. and Colwell, G.T., "Mathematical Modeling of the Transient Operating Characteristics of Low-Temperature Heat Pipes", Numerical Heat Transfer, Vol. 8, 1985, pp. 169-186.

7. Silverstein, C.C., "A Feasibility Study of Heat Pipe Cooled Leading Edges for Hypersonic Cruise Aircraft", NASA CR-1857, 1971.

8. Niblock, G., Reeder, J. and Huneidi, F., "Four Space Shuttle Wing Leading Edge Concepts", Journal of Spacecraft, Vol. 11, No. 5, 1974, pp. 314-320.

9. Camarda, C., "Analysis and Radiant Heating Tests of a Heat Pipe Cooled Leading Edge", NASA TN D-8468, 1977.

10. Camarda, C., "Aerothermal Tests of a Heat Pipe Cooled Leading Edge at Mach 7", NASA TP-1320, 1978.

11. Colwell, G.T., Jang, J. and Camarda, C., "Modeling of Startup from the Frozen State", Proceedings of the Sixth International Heat Pipe Conference, Grenoble, France, 1987, pp. 165-170.

12. Jang, J., "An Analysis of Startup from the Frozen State and Transient Performance of Heat Pipes", PhD Thesis, Georgia Institute of Technology, 1988.

13. Colwell, G.T., "Cooling Hypersonic Vehicle Structures", Proceedings of the Seventh International Heat Pipe Conference, Minsk, U.S.S.R., 1990.

14. Hendrix, W., "An Analysis of Body Force Effects on the Transient and Steady-State Performance of Heat Pipes", PhD Thesis, Georgia Institute of Technology, 1989.

15. Glass, D. and Camarda, C., "Results of Preliminary Design Studies of a Carbon-Carbon/Refractory Metal Heat Pipe Wing Leading Edge", Sixth National Aerospace Plane Symposium, 1989.

16. Silverstein, C.C., "Heat Pipe Cooling for SCRAMJET Engines", NASA CR-4036, 1986.

17. Silverstein, C.C., "Heat Pipe Cooling Systems with Sensible Heat Sink", Sandia National Laboratories Contract 33-0878, 1988.

18. Leadon, B. and Scott, C., "Transpiration Cooling Experiments in a Turbulent Boundary Layer at M=3", Journal of the Aeronautical Sciences, 1956.

19. Walton, T., Rashis, B. and Winters, C., "Free Flight Investigations of Subliming Ablators and Transpiration Cooling at Hypersonic Velocities", AIAA Vehicle Design and Propulsion Meeting, 1963.

20. Walton, T., "Free Flight Investigation of Mass Transfer Cooling on a Blunt Cone to a Mach Number of 10.6", NASA Langley Research Center, 1964.

21. Gollnick, A., "An Experimental Study of the Thermal Diffusion Effects on a Partially Porous Mass Transfer Cooled Hemisphere", International Journal of Heat and Mass Transfer, Vol. 7, 1964.

22. Roland, H., Pasqua, P. and Stevens, P., "Film and Transpiration Cooling of Nozzle Throats", AEDC-TR-66-88, 1966.

23. Redeker, E. and Miller, D., "Mach 16 Film Cooling", Proceedings of the 1966 Heat Transfer and Fluid Mechanics Institute, 1966.

24. Inger, G. and Sayano, S., "Effects of Gaseous Injection on the Hypersonic Flow Around Transpiration Cooled Bodies", Journal of Spacecraft, Vol. 6, No. 6, 1969.

25. Dunavant, J. and Mulligan, J., "Downstream Cooling Effectiveness of Massive Upstream Transpiration from a Slender Cone", AIAA Journal, Vol. 7, No. 9, 1969.

26. Dunavant, J. and Everhart, P., "Exploratory Heat Transfer Measurements at Mach 10 on a 7.5 Degree Total Angle Cone Downstream od a Region of Air and Helium Transpiration Cooling", NASA TN D-5554, 1969.

27. Gater, R., "A Discussion and Analysis of Some Aspects of Transpiration Cooled Nosetips", Air Force Report No. SAMSO-TR-70-80, 1969.

28. Schneider, P., Maurer, R. and Strapp, M., "Two Dimensional Transpiration Cooled Nosetip", Journal of Spacecraft, Vol. 8, No. 2, 1971.

29. Steurer, W., "Principles and Capabilities of Ablation", ASTM Special Technical Publication No. 279, 1959.

30. Camberos, J.A. and Roberts, L., "Analysis of Internal Ablation for the Thermal Control of Aerospace Vehicles", Joint Institute for Aeronautics and Acoustics, Stanford University, JIAA TR-94, Aug 1989.

31. Kelley, J. and L'Ecuyer, M., "Transpiration Cooling--Its Theory and Application", Purdue Research Foundation Report No. TM-66-5, 1966.

32. Hartnett, J. and Eckert, E., "Mass Transfer Cooling in a Laminar Boundary Layer with Constant Fluid Properties", Transactions of the ASME, Vol. 79, 1957.

33. Eckert, E., Schneider, P., Hayday, A. and Larson, R., "Mass Transfer Cooling of a Laminar Boundary Layer by Injection of a Light Weight Foreign Gas", Jet Propulsion, Vol. 28, 1958.

34. Tien, C. and Gee, C., "Hypersonic Viscous Flow Over a Sweat-Cooled Flat Plate", AIAA Journal, Vol. 1, No. 1, 1963.

35. Woodruff, L. and Lorenz, G., "Hypersonic Turbulent Transpiration Cooling Including Downstream Effects", AIAA Journal, Vol. 4, No. 6, 1966.

36. Schneider, P. and Maurer, R., "Coolant Starvation in a Transpiration Cooled Hemispherical Shell", Journal of Spacecraft, Vol. 5, No. 6, 1968.

37. Laganelli, A., "A Comparison Between Film Cooling and Transpiration Cooling Systems in High Speed Flow", AIAA Paper No. 70-153, 1970.

38. Parthasarathy, K. and Zakkay, V., "Turbulent Slot Injection Studies at Mach 6", Aerospace Research Laboratories ARL 69-0066, 1969.

39. Parthasarathy, K. and Zakkay, V., "An Experimental Investigation of Turbulent Slot Injection at Mach 6", AIAA Journal, Vol. 8, No. 7, 1970.

40. Cary, A. and Hefner, J., "Film Cooling Effectiveness in Hypersonic Turbulent Flow", AIAA Journal, Vol. 8, No. 11, 1970.

41. Laganelli, A. and Fogaroli, R., "Downstream Influence of Film-Cooling in a High Speed Laminar Boundary Layer", AIAA Paper No. 71-425, 1971.

42. Cary, A. and Hefner, J., "An Investigation of Film Cooling Effectiveness and Skin Friction in Hypersonic Turbulent Flow", AIAA Paper No. 71-599, 1971.

43. Miner, E. and Clark, L., "Supersonic Turbulent Boundary Layer Flows with Tangential Slot Injection", AIAA Paper No. 73-696, 1973.

44. Hefner, J. and Cary, A., "Swept Slot Film Cooling Effectiveness in Hypersonic Turbulent Flow", Journal of Spacecraft, Vol. 11, No. 5, 1974.

45. Starkenberg, J. and Cresci, R., "Boundary Layer Transition on a Film Cooled Slender Cone", AIAA Paper No. 75-194, 1975.

46. Robinson, A., McAlexander, R., Ramsdell, J. and Wolfson, M., "Transpiration Cooling with Liquid Metals", AIAA Journal, Vol. 1, No. 1, 1963.

47. Piva, R. and Strokowski, A., "Cross Flow Influence on Slot Cooling Effectiveness", Journal of Aircraft, Vol. 12, No. 7, 1975.

48. Murray, A. and Lewis, C., "Supersonic Turbulent Boundary Layer Flows with Mass Injection Through Slots and/or Porous Walls", NASA CR-2587, 1975.

49. Richards, B. and Stollery, J., "An Experimental Study of the Cooling Effectiveness of a Laminar Two Dimensional Tangential Film in Hypersonic Flow", AIAA Paper No. 77-703, 1977.

50. Cary, A., Bushnell, D. and Hefner, J., "Predicted Effects of Tangential Slot Injection on Turbulent Boundary Layer Flow Over a Wide Speed Range", Journal of Heat Transfer, Vol. 101, 1979.

51. Cresci, R. and Bloom, M., "Hypersonic and Other Viscous Interactions", AFSOR-TR-82-0890, 1982.

52. Banken, G., Roberts, D., Holcomb, J. and Birch, S., "A Parabolized Navier-Stokes Prediction of Hypersonic Window Cooling", Journal of Spacecraft, Vol. 23, No. 3, 1986.

53. Sharpe, L., "Development of Computer Models for Correlating Data of Film Cooling of Nose Cone Under Hypersonic Flow", NASA CR-180673, 1987.

54. Lees, L., "Laminar Heat Transfer Over Blunt Nosed Bodies at Hypersonic Flight Speeds", Jet Propulsion, Vol. 26, 1956.

55. Fay, J. and Riddell, F., "Theory of Stagnation Point Heat Transfer in Dissociated Air", Journal of the Aeronautical Sciences, Vol. 25, No. 2, 1958.

56. Van der Vegt, J., "Transition to Turbulence in Laminar Hypersonic Flow", Center for Turbulence Research, 1988.

57. Henline, W., "Transpiration Cooling of Hypersonic Blunt Bodies with Finite Rate Surface Reactions", NASA CR-177516, 1989.

58. Dechaumphai, P., Wieting, A. and Pandey, A., "Finite Element Flow-Thermal-Structural Analysis of Aerodynamically Heated Leading Edges", NASA Langley Research Center, 1989.

59. Schmidt, J.F., "Laminar Skin-Friction and Heat Transfer Parameters for a Flat Plate at Hypersonic Speeds in Terms of Free-Stream Flow Properties", NASA TN D-8, Sep 1959.

60. Gross, J., Hartnett, J., Masson, D. and Gazley, C., "A Review of Binary Laminar Boundary Layer Characteristics", International Journal of Heat and Mass Transfer, Vol. 3, 1961, pp. 198-221.

61. Swenson, B.L., "An Approximate Analysis of Film Cooling on Blunt Bodies by Gas Injection Near the Stagnation Point", NASA TN D-861, Sep 1961.

62. Eckert, E., "Engineering Relations for Heat Transfer and Friction in High-Velocity Laminar and Turbulent Boundary Layer Flows Over Surfaces with Constant Pressure and Temperature", Transactions of the ASME, Aug 1956.

63. Morkovin, M., "Critical Evaluation of Transition from Laminar to Turbulent Shear Layers with Emphasis on Hypersonically Traveling Bodies", AFFDL-TR-68-149, Mar 1969.

64. Cresci, R. and Starkenberg, J., "Liquid Film Cooling on Hypersonic Slender Bodies", Astronautica Acta, Vol. 18, 1973, pp. 11-20.

65. Leont'ev, A., "Heat and Mass Transfer in Turbulent Boundary Layers", Advances in Heat Transfer, ed. Irvine, T. and Hartnett, J., Vol. 3, 1966.

66. Zakkay, V. and Callahan, C., "Laminar, Transition, and Turbulent Heat Transfer to a Cone-Cylinder-Flare Body at Mach 8", Journal of Aerospace Sciences, Vol. 29, Dec 1962.

67. Levine, J., "Transpiration and Film Cooling Boundary Layer Computer Program, Vol. I", Final Report--Contract NAS7-791, N72-19312, Jun 1971.

68. Low, G., "The Compressible Laminar Boundary Layer with Fluid Injection", NACA TN 3404, Mar 1955.

69. Witte, W. and Rashis, B., "An Experimental Investigation and Correlation of the Heat Reduction to Nonporous Surfaces Behind a Porous Leading Edge Through Which Coolant is Ejected", NASA TM X-235, Mar 1960.

70. Miner, E. and Lewis, C., "A Finite Difference Method for Predicting Supersonic Turbulent Boundary Layer Flows with Tangential Slot Injection", NASA CR-2124, Oct 1972.

71. Murray, A. and Lewis, C., "Supersonic Turbulent Boundary Layer Flows with Mass Injection Through Slots and/or Porous Walls", NASA CR-2587, Sep 1975.

72. Hatch, J. and Papell, S., "Use of a Theoretical Flow Model to Correlate Data for Film Cooling or Heating an Adiabatic Wall by Tangential Injection of Gases of Different Fluid Properties", NASA TN D-130, Nov 1959.

73. Ledford, O. and Stollery, J., "Film Cooling of Hypersonic Inlets", I.C. Aero Report 72-15, Jul 1972.

74. McConarty, W. and Anthony, F., "Design and Evaluation of Active Cooling Systems for Mach 6 Cruise Vehicle Wings", NASA CR- 1916, 1971.

75. Tavella, D. and Roberts, L., "Transpiration Cooling in Hypersonic Flight", Joint Institute for Aeronautics and Acoustics, Stanford University, JIAA TR-92, Jun 1989.

76. Priester, D.E., "Transient Response of a Cryogenic Heat Pipe", MS Thesis, Georgia Institute of Technology, 1976.

77. Chang, W.S., "Heat Pipe Startup from the Supercritical State", PhD Thesis, Georgia Institute of Technology, 1981.

78. Hughes, J.D., "Development of a Rectangular Heat Pipe Model for Transient Performance Analysis", Special Problem Report, School of Mechanical Engineering, Georgia Institute of Technology, Dec 1988.

79. Camarda, C.J. and Masek, R.V., "Design, Analysis, and Tests of a Shuttle-Type Heat Pipe Cooled Leading Edge", AIAA Journal of Spacecraft and Rockets, Vol. 18, No. 1, 1981.

80. Morrison, J., "Auxiliary Cooling in Heat Pipe Cooled Hypersonic Wings", MS Thesis, Georgia Institute of Technology, 1990.

81. Anderson, J.D., Hypersonic and High Temperature Gas Dynamics, McGraw-Hill, New York, 1989, pp. 249-250.

82. Klunker, E.B. and McLean, F.E., "Laminar Friction and Heat Transfer at Mach Numbers from 1 to 10", NACA TN 2499, Oct 1951.

83. Reshotko, E. and Cohen, C., "Heat Transfer at the Forward Stagnation Point of Blunt Bodies", NACA TN 3513, Jul 1955.

84. Kemp, N.H., Rose, P.H. and Detra, R.W., "Laminar Heat Transfer Around Blunt Bodies in Dissociated Air", Journal of the Aero/Space Sciences, Jul 1959, pp. 421-430.

85. Sparrow, E.M., "Unsteady Stagnation-Point Heat Transfer", NASA TN D-77, Oct 1959.

86. Wisniewski, R.J., "Methods of Predicting Laminar Heat Transfer Rates on Hypersonic Vehicles", NASA TN D-201, Dec 1959.

87. Beckwith, I.E. and Gallagher, J.J., "Local Heat Transfer and Recovery Temperatures on a Yawed Cylinder at a Mach Number of 4.15 and High Reynolds Numbers", NASA TR R-104, 1962.

88. Huber, P.W., "Hypersonic Shock-Heated Flow Parameters for Velocities to 46,000 Feet Per Second and Altitudes to 323,000 Feet", NASA TR R-163, Dec 1963.

89. Richards, B., Dicristina, V. and Minges, M., "Heat Transfer and Pressure Distribution on Sharp and Finite Bluntness Biconic and Hemispherical Geometries at Various Angles of Attack in a Mach 15-20 Flow", Astronautical Research 1971, pp. 91-103.

90. Hamilton, H.H., "Calculation of Laminar Heating Rates on Three-Dimensional Configurations Using the Axisymmetric Analogue", NASA TP 1698, Sep 1980.

91. Zoby, E.V. and Simmonds, A.L., "Engineering Flowfield Method with Angle of Attack Applications", AIAA-84-0303, Jan 1984.

92. DeJarnette, F.R., Hamilton, H.H., Weilmuenster, K.J. and Cheatwood, F.M., "A Review of Some Approximate Methods Used in Aerodynamic Heating Analyses", Journal of Thermophysics and Heat Transfer, Vol. 1, No. 1, 1987, pp. 5-12.

93. Gnoffo, P.A., Gupta, R.N. and Shinn, J.L., "Conservation Equations and Physical Models for Hypersonic Air Flows in Thermal and Chemical Nonequilibrium", NASA TP 2867, 1989.

94. Tauber, M., Menees, G. and Adelman, H., "Aerothermodynamics of Transatmospheric Vehicles", Journal of Aircraft, Vol. 24, No. 9, 1987, pp. 594-602.

95. Yamamoto, Y., Arakawa, H. and Yoshida, R., "Numerical Simulation of Hypersonic Flow Around a Space Plane. III Analysis of Aerothermodynamic Heating", National Aerospace Laboratory, Tokyo, Japan, PB 90-255761, 1989.

96. Air Force Office of Scientific Research, "Analysis of Flow-, Thermal-, and Structural-Interaction of Hypersonic Structures Subjected to Severe Aerodynamic Heating", Annual Technical Report #2, TR-89-15, Feb 1990.

97. Hansen, C.F., "Approximations for the Thermodynamic and Transport Properties of High-Temperature Air", NACA TN 4150, 1958.

98. Wittliff, C.E. and Curtiss, J.T., "Normal Shock Wave Parameters in Equilibrium Air", Cornell Aeronautical Laboratory Report No. CAL-111, 1961.

99. Marrone, P.V., "Normal Shock Waves in Air: Equilibrium Composition and Flow Parameters for Velocities from 26,000 to 50,000 ft/s", Cornell Aeronautical Laboratory Report No. AG-1729-A-2, 1962.

100. Weast, R.C., ed., CRC Handbook of Chemistry and Physics, 64th Edition, CRC Press, Boca Raton, Florida, 1983.

101. Liepmann, H.W. and Roshko, A., Elements of Gasdynamics, John Wiley and Sons, New York, 1957, p. 326.

102. McComb, H., Murrow, H. and Card, M., "Structures and Materials Technology for Hypersonic Aerospacecraft", NASA TM-102583, Jan 1990.

103. Hallion, R., ed., "The Hypersonic Revolution: Eight Case Studies in the History of Hypersonic Technology, Volume II (1964-1986)", Aeronautical Systems Division, Wright-Patterson Air Force Base, 1987.

104. Edney, B., "Homologous Heat Transfer and Pressure Distributions on Blunt Bodies at Hypersonic Speeds in the Presence of Impinging Shock", FFA Report 115, Aeronautical Research Institute of Sweden, 1968.

105. Stewart, J., Thareja, R., Wieting, A. and Morgan, K., "Application of Finite Element and Remeshing Technique to Shock Interference on a Cylindrical Leading Edge", AIAA Paper No. 88-0368, Jan 1988.

106. Holden, M.S., Wieting, A.R., Moselle, J.R. and Glass, C., "Studies of Aerothermal Loads Generated in Regions of Shock/Shock Interaction in Hypersonic Flow", AIAA Paper No. 88-0477, Jan 1988.

107. Dechaumphai, P., Thornton, E. and Wieting, A., "Flow-Thermal-Structural Study of Aerodynamically Heated Leading Edges", AIAA Paper No. 88-2245-CP, Apr 1988.

108. Wieting, A. and Holden, M., "Experimental Shock-Wave Interference Heating on a Cylinder at Mach 6 and 8", AIAA Journal, Vol. 27, No. 11, 1989, pp. 1557-1565.

109. Liepmann, H.W. and Roshko, A., Elements of Gasdynamics, John Wiley and Sons, New York, 1957, pp. 85-88.

110. Glass, C., Holden, M. and Wieting, A., "Effect of Leading Edge Sweep on Shock-Shock Interference at Mach 8", AIAA Paper No. 89-0271, Jan 1989.

111. Hunt, J. and Martin, J., "Hypersonic Airbreathing Vehicle Conceptual Design (Focus on Aero-Space Plane)", NASA Langley Research Center, 1989.

112. Kinney, G.R., Abramson, A.F. and Sloop, J.L., "Internal-Liquid-Film-Cooling Experiments with Air-Stream Temperatures to 2000 Degree F in 2- and 4-Inch Diameter Horizontal Tubes", NACA Report 1087, 1952.

113. Gater, R.A. and L'Ecuyer, M.R., "A Fundamental Investigation of the Phenomena That Characterize Liquid-Film Cooling", Purdue University and Purdue Research Foundation Report No. TM-69-1, Jan 1969.

Other References Consulted

114. Adamson, T.C. and Howe, R.M., "Hypersonic Aerodynamics and Control Final Report", United States Army Strategic Defense Command Contract No. DASG60-88-C-0037, Jun 1990.

115. Buchmann, O.A., "Development and Fabrication of Structural Components for a SCRAMJET Engine", NASA CR 181945, Mar 1990.

116. Donaldson, J.C. and Sinclair, D.W., "Investigation of the Development of Laminar Boundary-Layer Instabilities Along a Cooled-Wall Hollow Cylinder at Mach Number 8", AEDC-TSR-89-V25, Jan 1990.

117. Clausen, R.D., "A Computational Model for Thickening Boundary Layers with Mass Addition for Hypersonic Engine Inlet Testing", MS Thesis, Air Force Institute of Technology, 1989.

118. Leingang, J.L., Donaldson, W.A., Watson, K.A. and Carreiro, L.R., "ETO--A Trajectory Program for Aerospace Vehicles", WRDC-TR-89-2023, Jun 1989.

119. Bowman, B., Citrin, K., Garner, E. and Stone, J., "Final Report Heat Pipes for Wing Leading Edges of Hypersonic Vehicles", McDonnell Aircraft Company Contract NAS1-18144, 1989.

120. Klopfer, G.H., Yee, H.C. and Kutler, P., "Numerical Study of Unsteady Viscous Hypersonic Blunt Body Flows with an Impinging Shock", NASA TM 100096, Apr 1988.

121. Kaufman, A., "Structural Analyses of Engine Wall Cooling Concepts and Materials", NASA Lewis Research Center, N88-22405, 1988.

122. White, F.M., Fluid Mechanics, Second Edition, McGraw-Hill, New York, 1986.

123. Holman, J.P., Heat Transfer, Sixth Edition, McGraw-Hill, New York, 1986.

124. Rohsenow, W.M., Hartnett, J.P. and Ganic, E.N., Handbook of Heat Transfer Applications, Second Edition, McGraw-Hill, New York, 1985.

125. Holden, M., "Studies of Transpiration Cooling, Surface Roughness and Entropy Swallowing in Transitional and Turbulent Boundary Layers Over Nose Tips", XXX Congress International Astronautical Federation, IAF-79-F-42, 1979.

126. Peeples, M.E., Reeder, J.C. and Sontag, K.E., "Thermostructural Applications of Heat Pipes", NASA CR-159096, 1979.

127. Laganelli, A.L. and Martellucci, A., "Experimental Surface and Boundary Layer Measurements in a Hypersonic Boundary Layer with Non-Uniform Blowing", AIAA Paper No. 74-699, 1974.

128. Newman, R.W. and Allen, R.W., "Compact Transpiration Cooling Systems", APL Technical Digest, Vol. 11, No. 5, 1972, pp. 13-21.

129. Eckert, E.R. and Drake, R.M., Analysis of Heat and Mass Transfer, McGraw-Hill, New York, 1972.

130. Becker, J.V., "Prospects for Actively Cooled Hypersonic Transports", Astronautics and Aeronautics, Aug 1971, pp. 32-39.

131. Miller, R.H., "Thinking Hypersonic", Astronautics and Aeronautics, Aug 1971, pp. 40-44.

132. Billig, F., "Shock-Wave Shapes Around Spherical- and Cylindrical-Nosed Bodies", Journal of Spacecraft, Vol. 4, No. 6, 1967.

133. Wolf, L., Obremski, H.J. and Christian, W.J., "Mass Transfer Cooling in Laminar Hypersonic Cavity Flow", AIAA Journal, Vol. 3, No. 6, 1965, pp. 1181-1182.

134. Dorrance, F., Viscous Hypersonic Flow, McGraw-Hill, New York, 1962.

135. Rashis, B., "Exploratory Investigation of Transpiration Cooling of a 40 Degree Double Wedge Using Nitrogen and Helium as Coolants at Stagnation Temperatures from 1,295 Degree F to 2,910 Degree F", NASA TN D-721, May 1961.

136. Howe, J.T. and Mersman, W.A., "Solutions of the Laminar Compressible Boundary-Layer Equations with Transpiration Which Are Applicable to the Stagnation Regions of Axisymmetric Blunt Bodies", NASA TN D-12, Aug 1959.

137. Rubesin, M.W., Pappas, C.C. and Okuno, A.F., "The Effect of Fluid Injection on the Compressible Turbulent Boundary Layer--Preliminary Tests on Transpiration Cooling of a Flat Plate at M=2.7 with Air as the Injected Gas", NACA RM A55I19, Dec 1955.

138. Chauvin, L.T. and Carter, H.S., "Exploratory Tests of Transpiration Cooling on a Porous 8 Degree Cone at M=2.05 Using Nitrogen Gas, Helium Gas, and Water as the Coolants", NACA RM L55C29, Jun 1955.

139. Eckert, E.R., "Transpiration and Film Cooling", Heat Transfer...a Symposium, Engineering Research Institute, University of Michigan, 1953, pp. 195-210.

140. Franklin, H.N., "Building a Better Heat Pipe", Mechanical Engineering, Aug 1990, pp. 52-54.

141. Selby, S.M., ed., CRC Standard Mathematical Tables, 21st Edition, The Chemical Rubber Co., Cleveland, Ohio, 1973.

VITA

James Michael Modlin was born in Long Beach, California on November 6, 1955. His parents are James K. and Pauline S. Modlin and his brother is John K. Modlin. He received his primary and secondary education in Bellflower, California, graduating from Bellflower High School in 1973. He attended the United States Military Academy at West Point from 1973 to 1977. In June 1977 he was awarded the degree of Bachelor of Science and was commissioned as a Second Lieutenant in the United States Army. Since that time he has served as an active duty commissioned officer in the Army and currently holds the rank of Major. While on active duty, he has served in numerous Army combat and construction engineer units. In 1981 he was registered as a professional engineer in the state of Virginia. From 1983 to 1985 he attended the Massachusetts Institute of Technology where he received the degrees of Mechanical Engineer and Master of Science in Mechanical Engineering. During the period from 1985 to 1988 he was assigned to the faculty of the United States Military Academy in the Department of Mechanics. There he served as an assistant professor teaching thermodynamics and heat transfer. In 1988, he began his doctoral studies at the Georgia Institute of Technology and was awarded the degree of Doctor of Philosophy in Mechanical Engineering in June 1991.

James Michael Modlin married Cynthia Anne Maslak of Terryville, Connecticut, in June 1977 and has four sons: James, Matthew, Daniel and Joshua.